Materials and Methods

Identification of gene fusions from whole transcriptome (RNA-seq) and exome sequencing

RNA-Sequencing was performed from total RNA extracted from GSC cultures isolated from nine GBM patients using Illumina HiSeq 2000, producing roughly 60.3 million paired reads per sample. Using the global alignment software Burrows-Wheeler Aligner (BWA) (*1*) with modified Mott's trimming, an initial seed length of 32, maximum edit distance of 2 and a maximum gap number of 1, on average 43.1 million reads were mapped properly to the RefSeq transcriptome and, of the remaining, 8.6 million were mapped to the hg19 genome per sample. We considered the remaining 14.3% of paired reads—including those that failed to map to either transcriptome or genome with proper forward-reverse (F-R) orientation, within expected insert size, and with minimal soft clipping (unmapped portions at the ends of a read)—to be appropriate for gene fusion analysis.

We constructed a novel computational pipeline called ***TX-Fuse*** that identifies two sources of evidence for the presence of a gene fusion: 1. *Split inserts*, in which each read of a mate pair maps entirely to one side of a breakpoint, and 2. Individual *split reads* that span a breakpoint. Split inserts are readily detected from BWA mapping. On the other hand, split reads demand precision alignment of smaller nucleotide stretches. To that end, our pipeline employs the local alignment package BLAST with word size of 20, identity cutoff of 95%, expectation cutoff of 10^{-4}, and soft filtering to map raw paired reads against the RefSeq transcriptome. From this procedure, we obtained a list of potential split reads that were

filtered to ensure maintenance of coding frame in the predicted fusion transcript given the proper F-R orientation in the read pair. We also screened out false positive candidates produced from paralogous gene pairs using the Duplicated Genes Database and the EnsemblCompara GeneTrees (*2*). Pseudogenes in the candidate list were annotated using the list from HUGO Gene Nomenclature Committee (HGNC) database (*3*) and given lower priority. For each remaining gene fusion candidate, we created a virtual reference based on the predicted fusion transcript and re-mapped all unmapped reads using BLAST with word size of 16, identity cutoff of 85%, query coverage greater than 85%, and expectation cutoff of 10^{-4} to obtain a final count of split reads and inserts. Moreover, sequencing depth per base of the virtual reference was calculated to corroborate that components of each gene participating in the gene fusion were highly expressed.

To establish the recurrence of our initial panel of gene fusion candidates, we modified our gene fusion discovery pipeline to produce ***EXome-Fuse***, which probes for fusions within the available dataset of paired-read exome DNA sequencing of 336 matched GBM samples from TCGA. To increase sensitivity for gene fusion identification, we aligned reads unmapped by BWA to the gene pair participating in each fusion candidate using a BLAST word size of 24 for split inserts and 16 for split read and split insert discovery. Given that the breakpoint detected in DNA cannot directly indicate the resulting breakpoint in the transcribed RNA, we could not ensure fusion candidates to maintain coding frame. Moreover, we made no restriction on split insert orientation. For split reads, we only required that the component of the split read mapped to the same gene as its mate maintained F-R directionality.

Co-outlier expression and CNV analysis from Atlas-TCGA GBM samples

Tomlins et al. (*4*) reported that outlier gene expression from microarray datasets identifies candidate oncogenic gene fusions. Wang et al. (*5*) suggested a "breakpoint principle" for intragenic copy number aberrations in fusion partners. We combined the two principles (outlier expression and intragenic CNV) to identify candidate gene fusions in GBM samples from Atlas-TCGA. Genomic and expression data sets were downloaded from TCGA public data portal as available on December 1, 2011, where a description of TCGA data types, platforms, and analyses is also available (*6*). Specific data sources were (according to Data Levels and Data Types) as follows: Expression data, "Level 2" normalized signals per probe set (Affymetrix HT_HG-U133A) of 526 samples; Copy number data, "Level 1" raw signals per probe (Affymetrix Genome-Wide Human SNP *Array* 6.0) of 1070 samples (tumor and matched normal control).

The gene expression analysis was performed first using R (*7*). We calculated the median absolute deviation (MAD) and then we labeled a gene as an outlier according to the following formula: $Z_{i,j} = 0.6745(x_{i,j} - \text{mean}(x_i))/MAD_i > 3.5$ (*8*). Samples were identified as ECFS (expression candidate fusion sample) if both genes of interest (e. g. FGFR3 and TACC3) displayed outlier behavior (co-outliers). Next, ECFS were analyzed for CNV using pennCNV (*9*). Tumors samples were paired to their normal controls to obtain the log ratio values and the VEGA algorithm was used to obtain a more accurate segmentation (*10*). If genomic aberrations are revealed, the samples are identified as GECFS (genomic and

expression candidate fusion sample). The GBM samples TCGA-27-1835, TCGA-19-5958, TCGA-06-6390, TCGA-12-0826 were identified as GECFS for FGFR3-TACC3.

Cell culture and isolation and culture of GSCs

Rat1A, mouse astrocytes *Ink4A;Arf-/-*, Balb 3T3 and human astrocytes were cultured in DMEM supplemented with 10% Fetal Bovine Serum. Specimens of newly diagnosed GBM were dissociated using the Papain Dissociation System (Worthington Biomedical Corporation). Cells were grown in neurobasal medium (Invitrogen) supplemented with B27, N2 (Invitrogen), EGF (50 ng/ml, PeproTech) and FGF2 (50 ng/ml, PeproTech) to establish gliomasphere cultures enriched for GSCs. For treatment *in vitro* with PD173074, AZD4547 or BJG398 cells infected with vector control, FGFR3, TACC3, FGFR-TACC fusions or FGFR3-TACC3-K508M were seeded in 96-well plates and treated with increasing concentrations of FGFR inhibitors. After 72-120 h, cell viability measured using the 3-(4,5-dimethythiazol-2-yl)-2,5-diphenyl tetrazolium bromide (MTT) assay. Data were expressed as mean±SD. Growth rate in GSC-1123 infected with sh-Ctr or shRNA lentiviruses targeting FGFR3 was determined by plating dissociated gliomaspheres at $2x10^4$ cells/well in twelve-well plates post 5 days of infection. The number of viable cells was determined by trypan blue exclusion in triplicate cultures obtained from triplicate independent infections. Cell number was scored every other day.

Karyotyping

Cultured cells were treated with 0.02 µg/ml colcemid for 90 minutes at 37°C. The cells were then trypsinized, centrifuged for 7 minutes at 200 x g, and the cell pellet re-suspended in warmed hypotonic solution and incubated at 37°C for 13 minutes. The swollen cells were then centrifuged and the pellet re-suspended in 8 ml of Carnoy's fixative (3:1 methanol:glacial acetic acid). The cell suspension was centrifuged and washed twice in Carnoy's fixative. After the last centrifugation, the cells were resuspended in 0.5 to 1 ml of freshly prepared fixative to produce an opalescent cell suspension. Drops of the final cell suspension were placed on clean slides and air-dried. Slides were stained with DAPI and metaphases were analyzed under a fluorescent microscope. At least 100 cells in metaphase were examined for chromosome count. PMSCS was scored in cells where a majority of the sister chromosomes were no longer associated. Two-tailed unpaired t-tests with Welch's correction were performed for comparison of means analysis.

Genomic and mRNA RT-PCR

Total RNA was extracted from cells by using RNeasy Mini Kit (QIAGEN), following the manufacturer instructions. 500 ng of total RNA was retro-transcribed by using the Superscript III kit (Invitrogen), following the manufacturer instructions. The cDNAs obtained after the retro-transcription was used as templates for qPCR as described (*11, 12*). The reaction was performed with a Roche480 thermal cycler, using the Absolute Blue QPCR SYBR Green Mix from Thermo Scientific. The relative amount of specific mRNA was normalized to 18S. Results are presented as the mean±SD of triplicate amplifications. The validation of fusion transcripts was performed using both genomic and RT-PCR with

forward and reverse primer combinations designed within the margins of the paired-end read sequences detected by RNA-seq. To identify novel fusion transcripts within the GBM cohort, PCR primers pairs were designed to bind upstream to the TK domain of the FGFR genes and inside or downstream of the Coiled Coil domain of the TACC genes. Expressed fusion transcript variants were subjected to direct sequencing to confirm sequence and translation frame. Primers used are:

hFGFR3-RT-FW1: 5'-GTAACCTGCGGGAGTTTCTG-3';

hFGFR3-RT-REV1: 5'-ACACCAGGTCCTTGAAGGTG-3';

hTACC3-RT-FW2: 5'-CCTGAGGGACAGTCCTGGTA-3';

hTACC3-RT-REV2: 5'-AGTGCTCCCAAGAAATCGAA-3';

hWRAP53-RT-FW1: 5'-AGAGGTGACCACCAATCAGC-3';

hWRAP53-RT-REV1: 5'-CGTGTCCCACACAGAGACAG-3';

Primers used for the screening of FGFR-TACC fusions are:

FGFR3-FW1: 5'-CGTGAAGATGCTGAAAGACGATG-3';

TACC3-REV1: 5'- AAACGCTTGAAGAGGTCGGAG-3';

FGFR1-FW1: 5'-ATGCTAGCAGGGGTCTCTGA-3';

TACC1-REV1: 5'-CCCTTCCAGAACACCTTTCA-3';

Primers used for genomic detection of FGFR3-TACC3 fusion in GBM-1123 and GSC-1123 are:

genomicFGFR3-FW1: 5'-ATGATCATGCGGGAGTGC-3';

genomicTACC3-REV1: 5'-GGGGGTCGAACTTGAGGTAT-3';

Primers used to validate fusions detected by RNA-seq are:

POLR2A-FW1: 5'-CGCAGGCTTTTTGTAGTGAG-3';

WRAP53-REV1: 5'-TGTAGGCGCGAAAGGAAG-3';

PIGU-FW1: 5'-GAACTCATCCGGACCCCTAT-3';

NCOA6-REV1: 5'-GCTTTCCCCATTGCACTTTA-3';

ST8SIA4-FW1: 5'-GAGGAGAGAAGCACGTGGAG-3';

PAM-REV1: 5'-GGCAGACGTGTGAGGTGTAA-3';

CAPZB-FW: 5'-GTGATCAGCAGCTGGACTGT-3';

UBR4-REV1: 5'-GAGCCTGGGCATGGATCT-5';

Cloning and Lentiviral production

Lentiviral expression vectors, pLOC-GFP (Open Biosystems) and pTomo-shp53, were used to clone FGFR3, TACC3, FGFR3-TACC3, FGFR3-TACC3-K508M, and FGFR1-TACC1. pTomo-shp53 was a gift of Inder Verma and Dinorah Friedman-Morvinski (Salk Institute, San Diego). The FGFR3-TACC3-K508M mutant was generated using the Phusion Site Direct Mutagenesis kit (NEB, USA). MISSION shRNAs clones (pLKO.1 lentiviral expression vectors) against FGFR3 were purchased from Sigma. The hairpin sequences targeting the *FGFR3* gene are-

5′-TGCGTCGTGGAGAACAAGTTT-3′ (#TRCN0000000372; Sh#2);

5′-GTTCCACTGCAAGGTGTACAG-3′ (#TRCN0000430673; Sh#3);

5′-GCACAACCTCGACTACTACAA-3′ (#TRCN0000000374; Sh#4).

Subcutaneous xenografts and drug treatment

Rat1A or *Ink4A;Arf-/-* astrocytes ($5x10^5$) transduced with different lentiviral constructs were suspended in 150 µl of PBS, together with 30 µl of Matrigel (BD Biosciences), and injected

subcutaneously in the flank of athymic nude (Nu/Nu) mice (Charles River Laboratories, Wilmington, MA). For experiments with FGFR inhibitors, mice carrying ~200-300 mm^3 subcutaneous tumors derived from *Ink4A;Arf-/-* astrocytes were randomized to receive 50 mg/kg PD173074 in 0.05 M lactate buffer (pH 5) or an equal volume of lactate buffer by oral gavage. Treatment was administered for three cycles consisting of four consecutive days followed by two days of rest. Tumor diameters were measured with caliper, and tumor volumes estimated using the formula: 0.5 x length x $width^2$. Data are expressed as mean±SE. Mice were sacrificed when tumors in the control group reached the maximal size allowed by the IACUC Committee at Columbia University.

Orthotopic transplantation and drug treatment

Ink4A;Arf-/- astrocytes carrying a luciferase expressing vector were transduced with FGFR3-TACC3 lentivitus. $1x10^3$ cells in 2 μl of saline were injected in the caudate-putamen of 4-6 week old male athymic nude (Nu/Nu) mice using a stereotaxic frame (coordinates relative to bregma: 0.5 mm anterior; 1.1 mm lateral; 3.0 mm ventral) and a 26 gauge Hamilton syringe. Six days after injection, mice underwent bioluminescence imaging using a Xenogen CCD apparatus and were randomized to receive 50 mg/kg AZD4547 in 1% Tween 80 (treatment group) or DMSO in an equal volume of vehicle (control group) by oral gavage. AZD4547 was administered daily for two cycles of 10 days with a two day interval. Mice were monitored daily and sacrificed when neurological symptoms appeared. Kaplan-Meier survival curve was generated using the DNA Statview software package (AbacusConcepts, Berkeley, CA). Log-rank analysis was performed on the Kaplan-Meier

survival curve to determine statistical significance.

Intracranial injections of lentiviruses

Intracranial injection of FGFR3-TACC3-shp53, EGFRvIII-shp53 or shp53 pTomo lentiviruses was performed in 4 week-old C57BL/6J mice in accordance with guidelines of IACUC Committee. Briefly, 1.8 μl of purified lentiviral particles in PBS ($1X10^9$/ml) were injected into the dentate gyrus using a stereotaxic frame (coordinates relative to bregma: 1.45 mm posterior; 1.65 mm lateral; 2.4 mm ventral) and a 26 gauge Hamilton syringe. Mice were monitored daily and sacrificed when neurological symptoms appeared. Mouse brain was analyzed histopathologically and by immunofluorescence.

Histology and immunostaining

Tissue preparation and immunohistochemistry on brain tumors and immunofluorescence staining were performed as previously described (*11-13*). Antibodies and concentrations used in immunofluorescence staining are:

Anti-Ki67	Rabbit	1:1000	Vector Labs
Anti-pHH3	Rabbit	1:500	Millipore
Anti-FGFR3	Mouse	1:1000	Santa Cruz
Anti-TACC3	Goat	1:1000	USBiological
Anti-α-tubulin	Mouse	1:1000	Sigma
Anti-Nestin	Mouse	1:1000	BD Pharmingen
Anti-Olig2	Rabbit	1:200	IBL
Anti-GFAP	Rabbit	1:200	Dako
Anti-ERK	Rabbit	1:1000	Cell Signaling
Anti-pERK	Rabbit	1:1000	Cell Signaling
Anti-FRS	Rabbit	1:250	Santa Cruz
Anti-pFRS	Rabbit	1:1000	Cell Signaling
Anti-AKT	Rabbit	1:1000	Cell Signaling
Anti-pAKT473	Rabbit	1:1000	Cell Signaling

Immunofluorescence and live-cell microscopy.

Immunofluorescence microscopy was performed on cells fixed with 4% para-formaldehyde (PFA) in PHEM (60 mM PIPES, 27 mM HEPES, 10 mM EGTA, 4 mM $MgSO_4$, pH 7.0). Cells were permeabilized using 1% Triton X 100. Mitotic spindles were visualized by anti-α-tubulin antibodies (Sigma). Secondary antibodies conjugated to Alexa Fluor-488/-594 (Molecular Probes) were used. All staining with multiple antibodies were performed in a sequential manner. DNA was stained by DAPI (Sigma). Fluorescence microscopy was performed on a Nikon A1R MP microscope. Images were recorded with a *Z*-optical spacing of 0.25 µm and analyzed using ImageJ software (National Institute of Health). For live-cell analyses, Rat1A cells infected with pLNCX-H2B retrovirus and transduced with lentiviral vector or FGFR3-TACC3 fusion were seeded in glass bottom dishes in phenol red free DMEM and followed by time-lapse microscopy using the Nikon A1R MP biostation at 37°C and 5% CO_2/95% air. Images with a *Z*-optical spacing of 1 µm were recorded every 4 min for 8 h. Images of unchallenged mitosis from early prophase until cytokinesis were further processed using ImageJ software. The time-point of nuclear envelope breakdown (NEB) was defined as the first frame showing loss of smooth appearance of chromatin and anaphase was the first frame when chromosome movement towards the poles became apparent. Nuclear envelope reconstitution (NER) was defined as the first frame showing nuclei decondensation. Box and whisker plots were calculated from image sequences from at least 50 recorded cells. Statistical analysis was performed using StatView software (AbacusConcepts, Berkeley, CA). Two-tailed unpaired t-tests with Welch's correction were performed for comparison of means analysis.

Supplementary References

1. H. Li, R. Durbin, Fast and accurate short read alignment with Burrows-Wheeler transform. *Bioinformatics* **25**, 1754 (2009).

2. A. J. Vilella *et al.*, EnsemblCompara GeneTrees: Complete, duplication-aware phylogenetic trees in vertebrates. *Genome Res.* **19**, 327 (2009).

3. R. L. Seal, S. M. Gordon, M. J. Lush, M. W. Wright, E. A. Bruford, genenames.org: the HGNC resources in 2011. *Nucleic Acids Res.* **39**, D514 (2011).

4. S. A. Tomlins *et al.*, Recurrent fusion of TMPRSS2 and ETS transcription factor genes in prostate cancer. *Science* **310**, 644 (2005).

5. X. S. Wang *et al.*, An integrative approach to reveal driver gene fusions from paired-end sequencing data in cancer. *Nat. Biotechnol.* **27**, 1005 (2009).

6. Comprehensive genomic characterization defines human glioblastoma genes and core pathways. *Nature* **455**, 1061 (2008).

7. R: A Language and Environment for Statistical Computing. R Development Core Team (2011).

8. B. Iglewicz, D. C. Hoaglin, *How to detect and handle outliers*. (ASQC, Milwaukee, Wis., 1993).

9. K. Wang *et al.*, PennCNV: an integrated hidden Markov model designed for high-resolution copy number variation detection in whole-genome SNP genotyping data. *Genome Res.* **17**, 1665 (2007).

10. S. Morganella, L. Cerulo, G. Viglietto, M. Ceccarelli, VEGA: variational segmentation for copy number detection. *Bioinformatics* **26**, 3020 (2010).

11. M. S. Carro *et al.*, The transcriptional network for mesenchymal transformation of brain tumours. *Nature* **463**, 318 (2010).

12. X. Zhao *et al.*, The HECT-domain ubiquitin ligase Huwe1 controls neural differentiation and proliferation by destabilizing the N-Myc oncoprotein. *Nat. Cell Biol.* **10**, 643 (2008).

13. X. Zhao *et al.*, The N-Myc-DLL3 cascade is suppressed by the ubiquitin ligase Huwe1 to inhibit proliferation and promote neurogenesis in the developing brain. *Dev. Cell* **17**, 210 (2009).

Supplementary Figure Legends

Fig. S1

Identification and validation of gene fusions in GBM. **(A)** TX-Fuse pipeline for the identification of fusion transcripts from RNA-Seq data. **(B)** RT-PCR for *POLR2A-WRAP53* (left panel). Sanger sequencing chromatograms show the reading frames at the breakpoint and putative translation of the fusion proteins in the positive sample (right panel). **(C)** RT-PCR for *CAPZB-UBR4* (left panel). Sanger sequencing chromatograms show the reading frames at the breakpoint and putative translation of the fusion proteins in the positive sample (right panel). **(D)** RT-PCR for *ST8SIA4-PAM* (left panel). Sanger sequencing chromatograms show the reading frames at the breakpoint and putative translation of the fusion proteins in the positive sample (right panel). **(E)** RT-PCR for *PIGU-NCOA6* (right panel). Sanger sequencing chromatograms show the reading frames at the breakpoint and putative translation of the fusion proteins in the positive sample (right panel).

Fig. S2

Analysis and validation of the expression of *FGFR3-TACC3* fused transcripts in GSCs and GBM samples. **(A)** Amino acid sequence of the FGFR3-TACC3 protein in GSC-1123. Residues corresponding to FGFR3 and TACC3 are shown in red and blue, respectively. The fusion protein joins the TK domain of FGFR3 to the TACC domain of TACC3. **(B)** Expression measured by read depth from RNA-seq data. Grey arcs indicate predicted components of transcripts fused together. Overall read depth (blue) and split insert depth (red) are depicted in

the graph, with a 50-read increment and a maximum range of 1800 reads. Note the very high level of expression in the regions of the genes implicated in the fusion events, particularly for *FGFR3-TACC3*. **(C)** qRT-PCR shows very high expression of *FGFR3* and *TACC3* mRNA sequences included in the *FGFR3-TACC3* fusion transcript in GSC-1123. **(D)** Western blot analysis with a monoclonal antibody, which recognizes the N-terminal region of human FGFR3, shows expression of a ~150 kD protein in GSC-1123 but not in GSC-0331 and GSC-0114 that lack the *FGFR3-TACC3* rearrangement. **(E)** Immunostaining analysis with the FGFR3 antibody of the GBM-1123 (upper panels) and a GBM sample lacking the *FGFR3-TACC3* rearrangement (lower panels). FGFR3 (red), DNA (DAPI, blue). The pictures were taken at low (left) and high (right) magnification. **(F)** MS/MS analysis of ~150 kD fusion protein immunoprecipitated by the monoclonal anti-FGFR3 antibody from GSC-1123 identifies three unique peptides mapping to the FGFR3 (upper panels) and three peptides mapping to the C-terminal region of TACC3 (lower panels).

Fig. S3

Analysis of expression and CNV for the *FGFR3* and *TACC3* genes in TCGA derived GBM samples. **(A)** Co-outlier expression of *FGFR3* and *TACC3* in four GBM harboring *FGFR3-TACC3* gene fusions. **(B)** CNV analysis showing micro-amplifications of the rearranged portions of the *FGFR3* and *TACC3* genes in all four GBM samples harboring *FGFR3-TACC3* gene fusions. **(C)** Exome-Fuse pipeline for the identification of gene fusion rearrangements from DNA exome sequences.

Fig. S4

FGFR-TACC gene fusions identified by exome sequencing analysis. **(A)** Split-reads aligning to the genomic breakpoints of *FGFR3* and *TACC3* genes in four TCGA-GBM samples carrying gene fusions between *FGFR3* and *TACC3* genes. **(B-C)** *FGFR3-TACC3*-specific RT-PCR (left panel). Sanger sequencing chromatograms showing the reading frame at the breakpoint and putative translation of the fusion protein in the positive sample (right panel). **(D)** *FGFR1-TACC1*-specific RT-PCR from GBM samples (left panel). Sanger sequencing chromatograms showing the reading frame at the breakpoint and putative translation of the fusion protein in the positive samples (right panel). **(E)** *FGFR3-TACC3*-specific RT-PCR (left panel). Sanger sequencing chromatograms showing the reading frame at the breakpoint and putative translation of the fusion protein in the positive samples (right panel).

Fig. S5

Analysis of FGFR3-TACC3 fusion protein in cell lines and tumors **(A)** Rat1A cells transduced with control lentivirus or lentivirus expressing FGFR3, TACC3 or FGFR3-TACC3 were analyzed by Western blot with an antibody recognizing the N-terminus of FGFR3 (included in the FGFR3-TACC3 fusion protein) or the N-terminus of TACC3 (not included in the FGFR3-TACC3 fusion protein). **(B)** Quantitative Western blot of endogenous FGFR3-TACC3 in GSC-1123 compared with lentivirally expressed FGFR3-TACC3 in Rat1A. **(C)** Quantitative Western blot of ectopic FGFR3-TACC3 fusion protein in mouse *Ink4A;Arf-/-* astrocytes and mouse GBM (mGBM-15 and mGBM-17) compared with the endogenous expression in GSC-1123. **(D)** Western blot analysis of FGFR3-TACC3 and FGFR3-TACC3-K508M in Rat1A. **(E)** Subcutaneous tumors are

generated by *Ink4A;Arf-/-* astrocytes expressing FGFR-TACC fusions. Immunostaining of tumors from mice injected with *Ink4A;Arf-/-* astrocytes expressing FGFR3-TACC3 shows positivity for glioma-specific (Nestin, Olig2 and GFAP) and proliferation (Ki67 and pHH3) markers. **(F)** FGFR3 immunostaining of GBM-1123, GSC-1123, mouse GBM induced by FGFR3-TACC3 expressing lentivirus and subcutaneous xenograft of mouse astrocytes transformed by FGFR3-TACC3 fusion. FGFR3-TACC3, red; DNA (DAPI), blue. **(G)** Quantification of FGFR3-TACC3 positive cells in the tumors and cultures of cells shown in panel F. α-tubulin or β-actin are shown as control for loading. F3-T3: FGFR3-TACC3; F3-T3-K508M: FGFR3-TACC3-K508M.

Fig. S6

Analysis of FGFR signaling by FGFR3-TACC3 fusion protein. **(A-C)** *Ink4A;Arf-/-* mouse astrocytes transduced with different constructs were starved of mitogens and left untreated or treated with **(A)** FGF-2 (50 ng/ml) for the indicated times, **(B)** FGF-1 for 10 min at the indicated concentrations and **(C)** FGF-8 for 10 min at the indicated concentrations. Phospho-proteins and total proteins were analyzed by Western blot. β-actin and α-tubulin are shown as a control for loading. **(D)** Constitutive auto-phosphorylation of FGFR3-TACC3 fusion. Human astrocytes transduced with empty lentivirus or a lentivirus expressing FGFR3-TACC3 or FGFR3-TACC3-K508M were left untreated (0) or treated with 100 nM of the FGFR TK inhibitor PD173074 for the indicated times. Phospho-proteins and total proteins were analyzed by Western blot using the indicated antibodies. **(E)** Mouse GSCs derived from FGFR3-TACC3 or RasV12 induced glioma were left untreated (0) or treated with 100 nM of PD173074 for the indicated times.

Phospho-proteins and total proteins were analyzed by Western blot using the indicated antibodies. F3-T3: FGFR3-TACC3; F3-T3-K508M: FGFR3-TACC3-K508M.

Fig. S7

Z-stacked confocal images of the representative FGFR3-TACC3 expressing Ink4A;Arf-/- mouse astrocyte shown as a maximum intensity projection in Figure 3A. Cells were immunostained using FGFR3 (red) and α-tubulin (green). DNA was counterstained with DAPI (blue). Images were acquired at 0.250 μm intervals. Coordinates of the image series are indicated.

Fig. S8

Localization of FGFR3, TACC3 and FGFR3-TACC3 fusion in mitotic cells. **(A)** Maximum intensity projection confocal image of a representative FGFR3-TACC3 expressing *Ink4A;Arf-/-* mouse astrocyte at metaphase, immunostained using the FGFR3 antibody (red). FGFR3-TACC3 displays asymmetric localization on top of one spindle pole. **(B)** In telophase FGFR3-TACC3 localizes to the mid-body. **(C)** Maximum intensity projection confocal image of a representative TACC3 expressing *Ink4A;Arf-/-* mouse astrocyte at metaphase immunostained with the TACC3 antibody (red). TACC3 staining coincides with the spindle microtubules. **(D)** Maximum intensity projection confocal image of a representative FGFR3 expressing *Ink4A;Arf-/-* mouse astrocyte at metaphase immunostained with the FGFR3 antibody (red). FGFR3 does not show a distinct staining pattern in mitosis. Cells were co-immunostained using α-tubulin (green) to visualize the mitotic spindle. DNA was counterstained with DAPI (blue). Images were

acquired at 0.250 μm intervals. Endogenous levels of FGFR3 or TACC3 were undetectable under the applied experimental conditions. F3-T3: FGFR3-TACC3.

Fig. S9

FGFR3-TACC3 expression induces chromosome missegregation, chromatid cohesion defects, aneuploidy and defective spindle checkpoint. **(A)** Representative microphotographs of metaphase spreads from *Ink4A;Arf-/-* astrocytes expressing the empty vector or FGFR3-TACC3 fusion. Arrows indicate chromosome misalignments, lagging chromosomes and chromosome bridges. **(B)** Representative metaphase spreads show premature sister chromatid separation (PMSCS) in *Ink4A;Arf-/-* astrocytes expressing FGFR3-TACC3 (left panel). The number of mitosis with PMSCS was scored in at least 100 metaphases for each condition in three independent experiments (right panel). Data are presented as the means±standard deviation, (n=3). **(C)** Representative metaphase spreads show PMSCS in Rat1A cells expressing FGFR3-TACC3 fusion (left panel); the number of mitosis with PMSCS was scored in triplicate samples (right panel). Data are presented as the means±standard deviation, (n=3). **(D)** Nocodazole was added for the indicated times to Rat1A-H2B-GFP cells transduced with the specified lentiviruses. The mitotic index at each time point was determined by scoring the number of H2B-GFP-positive cells in mitosis at each time point. Data are presented as means±standard deviation, (n=3). **(E)** Karyotype analysis of Rat1A cells transduced with control, FGFR3, TACC3 or FGFR3-TACC3 expressing lentiviruses. Distribution of chromosome counts of cells arrested in mitosis and analyzed using DAPI. Chromosomes were counted in 100 metaphase cells for each condition to determine the ploidy and the diversity of chromosome counts within the cell

population. **(F)** Representative karyotypes of primary human astrocytes transduced with control or FGFR3-TACC3 expressing lentivirus. F3-T3: FGFR3-TACC3.

Fig. S10

Analysis of FGFR3-TACC3 fusion mediated growth alteration and specificity of FGFR TK inhibitor effects on cells carrying FGFR-TACC fusions. **(A)** Decreased proliferation is an early effect of FGFR3-TACC3 expression in human primary astrocytes (7 days after infection, passage 1). Values are the means±standard deviation, (n=4). **(B)** Enhanced proliferation rate of human primary astrocytes transduced with lentivirus expressing FGFR3-TACC3 fusion six weeks after infection (passage 10). Values are the means±standard deviation, (n=4). **(C-D)** Cell growth as determined by MTT assay for Rat1A cells transduced with the specified lentiviruses and subsequently treated for three days with vehicle or BGJ398 **(C)** or AZD4547 **(D)** at the indicated concentration. Values are the means±standard error of the ratio between inhibitor treated and vehicle treated cells, (n=4). **(E)** Rat1A cells expressing FGFR3-TACC3 fusion were transduced with lentivirus expressing a non-targeting shRNA (sh-Ctr) or shRNA sequences targeting FGFR3. Five days after infection, cell lysates were assayed by Western blot (left panel). The proliferation rate of parallel cultures was analyzed by the MTT assay at the indicated times. Infection with lentivirus expressing the most efficient FGFR3 silencing sequences (sh-3 and sh-4), reverted the growth of FGFR3-TACC3 expressing cultures to a rate comparable to that of Rat1A transduced with empty vector (right panel). Values are the means±standard deviation, (n=4). **(F)** GSC-1123 cells were transduced with lentivirus expressing a non-targeting shRNA (sh-Ctr) or lentivirus expressing sh-3 and sh-4 sequences

targeting FGFR3. Western Blot analysis was performed using the FGFR3 antibody to the detect FGFT3-TACC3 fusion protein (left panel). Parallel cultures of GSC-1123 cells were transduced in triplicate. Five days after infection cells were plated at density of $2X10^4$ cells/well in triplicate and the number of trypan blue excluding cells was scored at the indicated times (right panel). Values are the means± standard deviation, (n=3). **(G)** The FGFR TK inhibitor PD173074 suppresses tumor growth of subcutaneous tumors generated by *Ink4A;Arf-/-* astrocytes expressing FGFR3-TACC3. After tumor establishment (200-300 mm^3, arrow) mice were treated with vehicle or PD173074 (50 mg/kg) for 14 days. Values are mean tumor volumes±standard error, (n=7 mice per group).

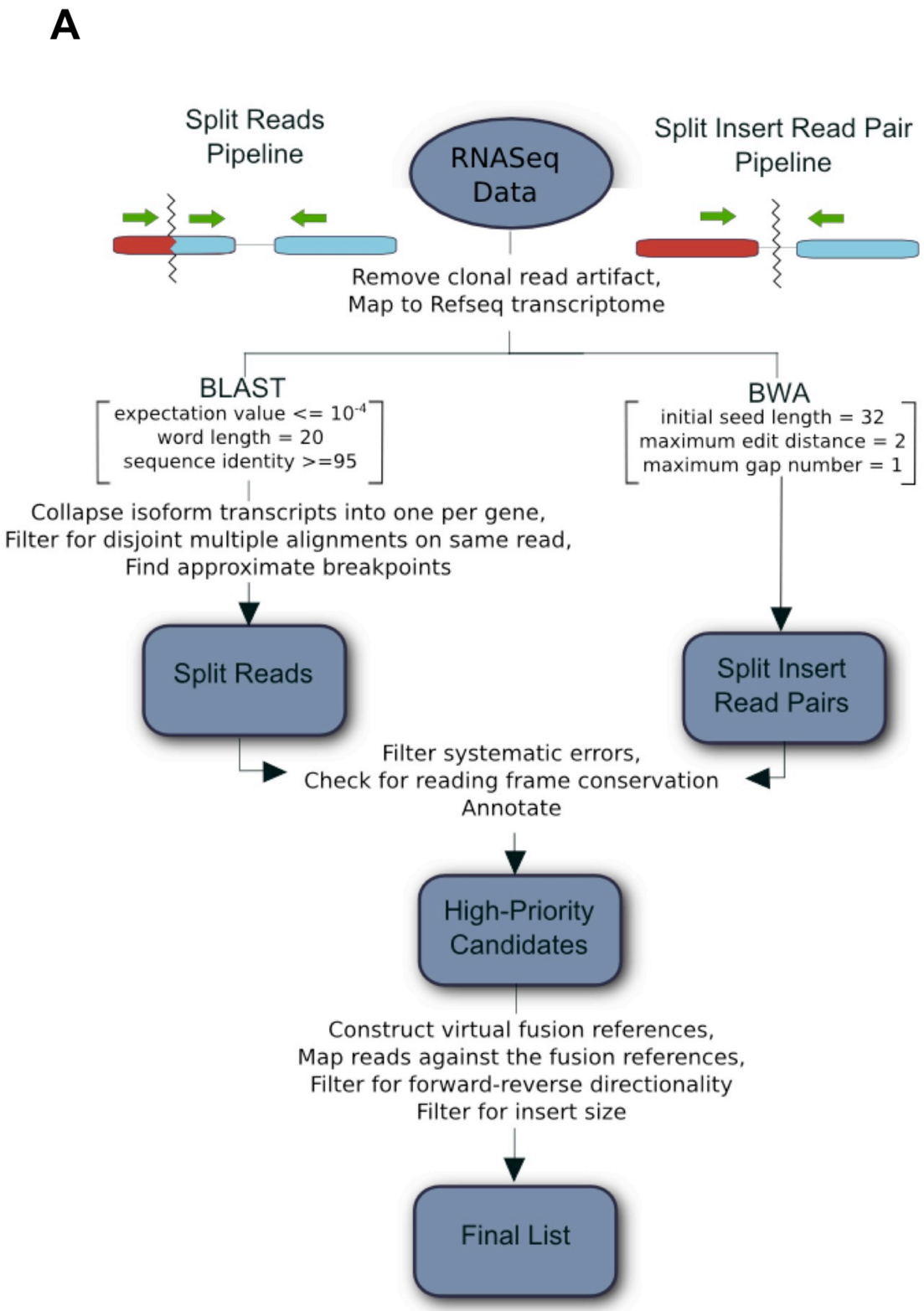
A
Split Reads Pipeline
RNASeq Data
Split Insert Read Pair Pipeline
Remove clonal read artifact,
Map to Refseq transcriptome
BLAST
expectation value <= 10-4
word length = 20
sequence identity >=95
BWA
initial seed length = 32
maximum edit distance = 2
maximum gap number = 1
Collapse isoform transcripts into one per gene,
Filter for disjoint multiple alignments on same read,
Find approximate breakpoints
Split Reads
Split Insert Read Pairs
Filter systematic errors,
Check for reading frame conservation
Annotate
High-Priority Candidates
Construct virtual fusion references,
Map reads against the fusion references,
Filter for forward-reverse directionality
Filter for insert size
Final List

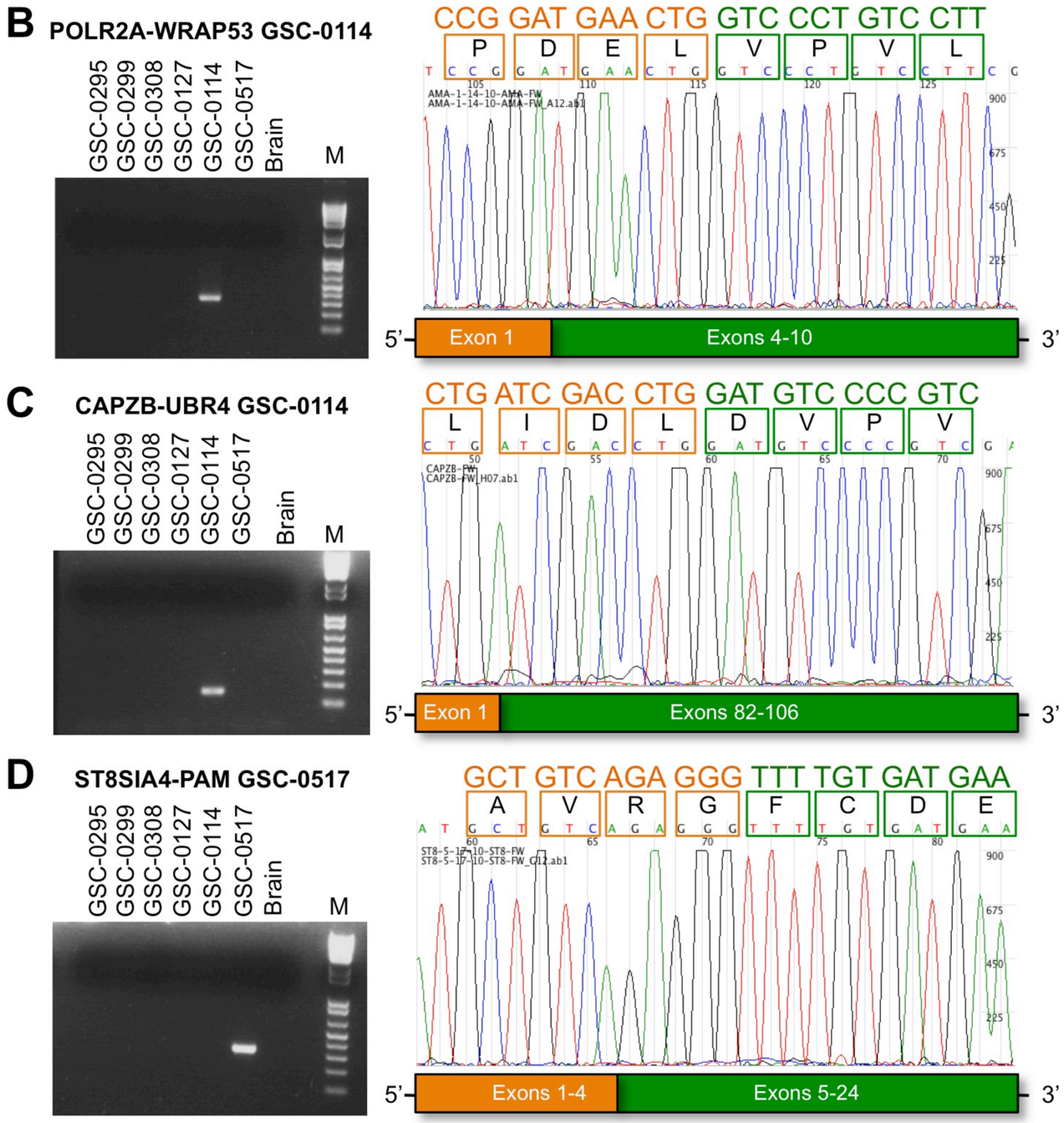
B
POLR2A-WRAP53 GSC-0114
GSC-0295
GSC-0299
GSC-0308
GSC-0127
GSC-0114
GSC-0517
Brain
M
CCG GAT GAA CTG GTC CCT GTC CTT
P D E L V P V L
5'
Exon 1
Exons 4-10
3'
C
CAPZB-UBR4 GSC-0114
CTG ATC GAC CTG GAT GTC CCC GTC
L I D L D V P V
Exons 82-106
D
ST8SIA4-PAM GSC-0517
GCT GTC AGA GGG TTT TGT GAT GAA
A V R G F C D E
Exons 1-4
Exons 5-24
E
PIGU-NCOA6 GSC-0308
TAC GAT AAA AGA CAT AAC CAG TGC
Y D K R H N Q C
Exons 1-6
Exon 16

Figure S1

A

```
MGAPACALALCVAVAIVAGASSESLGTEQRVVGRAAEVPGPEPGQQEQLV  50
FGSGDAVELSCPPPGGGPMGPTVWVKDGTGLVPSERVLVGPQRLQVLNAS 100
HEDSGAYSCRQRLTQRVLCHFSVRVTDAPSSGDDEDGEDEAEDTGVDTGA 150
PYWTRPERMDKKLLAVPAANTVRFRCPAAGNPTPSISWLKNGREFRGEHR 200
IGGIKLRHQQWSLVMESVVPSDRGNYTCVVENKFGSIRQTYTLDVLERSP 250
HRPILQAGLPANQTAVLGSDVEFHCKVYSDAQPHIQWLKHVEVNGSKVGP 300
DGTPYVTVLKTAGANTTDKELEVLSLHNVTFEDAGEYTCLAGNSIGFSHH 350
SAWLVVLPAEEELVEADEAGSVYAGILSYGVGFFLFILVVAAVTLCRLRS 400
PPKKGLGSPTVHKISRFPLKRQVSLESNASMSSNTPLVRIARLSSGEGPT 450
LANVSELELPADPKWELSRARLTLGKPLGEGCFGQVVMAEAIGIDKDRAA 500
KPVTVAVKMLKDDATDKDLSDLVSEMEMMKMIGKHKNIINLLGACTQGGP 550
LYVLVEYAAKGNLREFLRARRPPGLDYSFDTCKPPEEQLTFKDLVSCAYQ 600
VARGMEYLASQKCIHRDLAARNVLVTEDNVMKIADFGLARDVHNLDYYKK 650
TTNGRLPVKWMAPEALFDRVYTHQSDVWSFGVLLWEIFTLGGSPYPGIPV 700
EELFKLLKEGHRMDKPANCTHDLYMIMRECWHAAPSQRPTFKQLVEDLDR 750
VLTVTSTDFKESALRKQSLYLKFDPLLRDSPGRPVPVATETSSMHGANET 800
PSGRPREAKLVEFDFLGALDIPVPGPPPGVPAPGGPPLSTGPIVDLLQYS 850
QKDLDAVVKATQEENRELRSRCEELHGKNLELGKIMDRFEEVVYQAMEEV 900
QKQKELSKAEIQKVLKEKDQLTTDLNSMEKSFSDLFKRFEKQKEVIEGYR 950
KNEESLKKCVEDYLARITQEGQRYQALKAHAEEKLQLANEEIAQVRSKAQ1000
AEALALQASLRKEQMRIQSLEKTVEQKTKENEELTRICDDLISKMEKI   1048
```

B

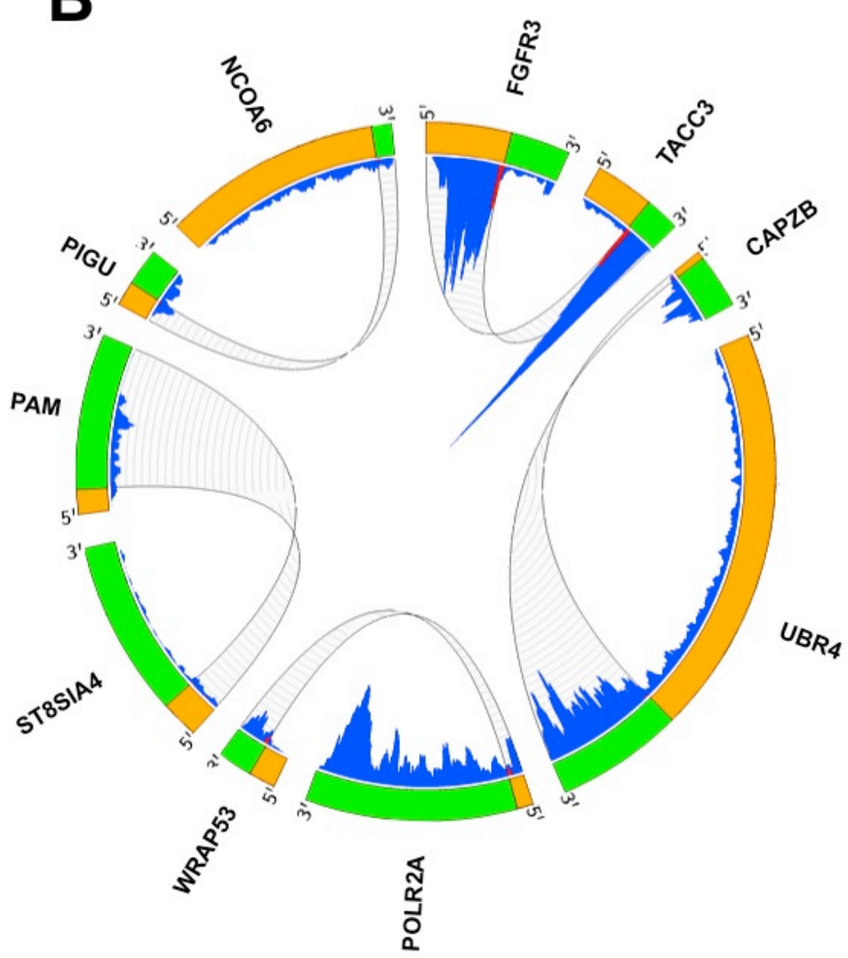

C

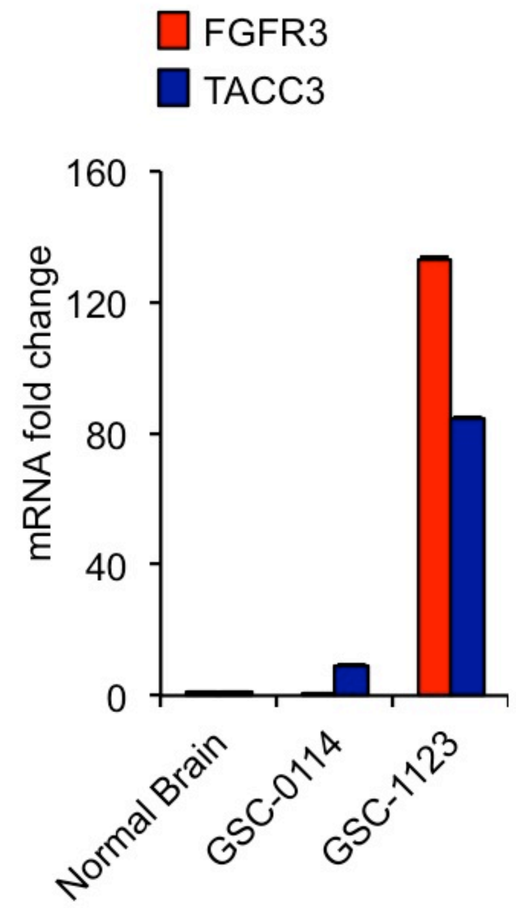

D

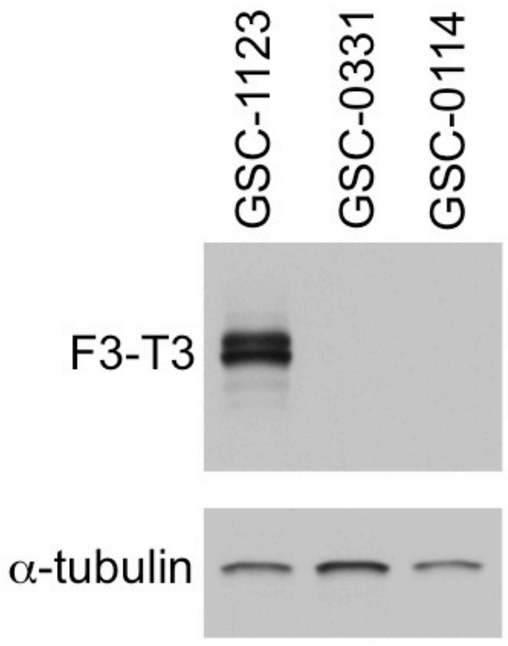

E

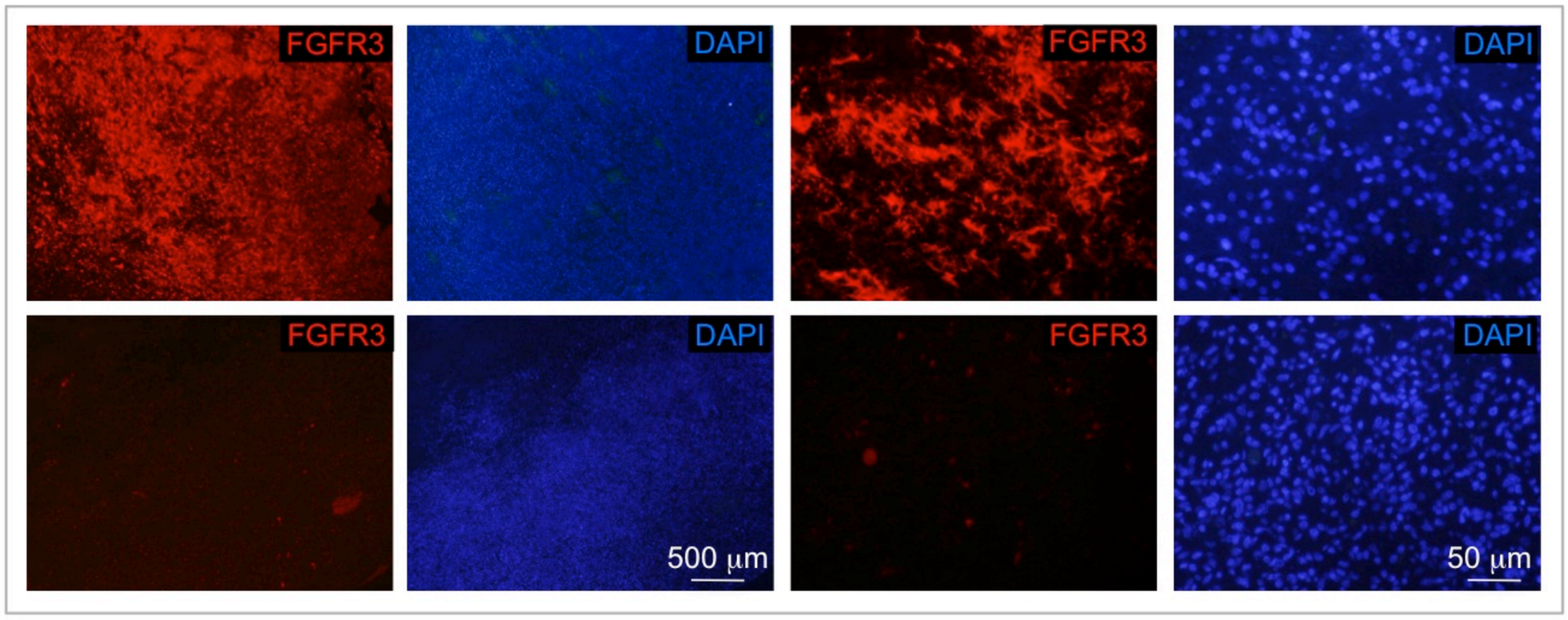

F

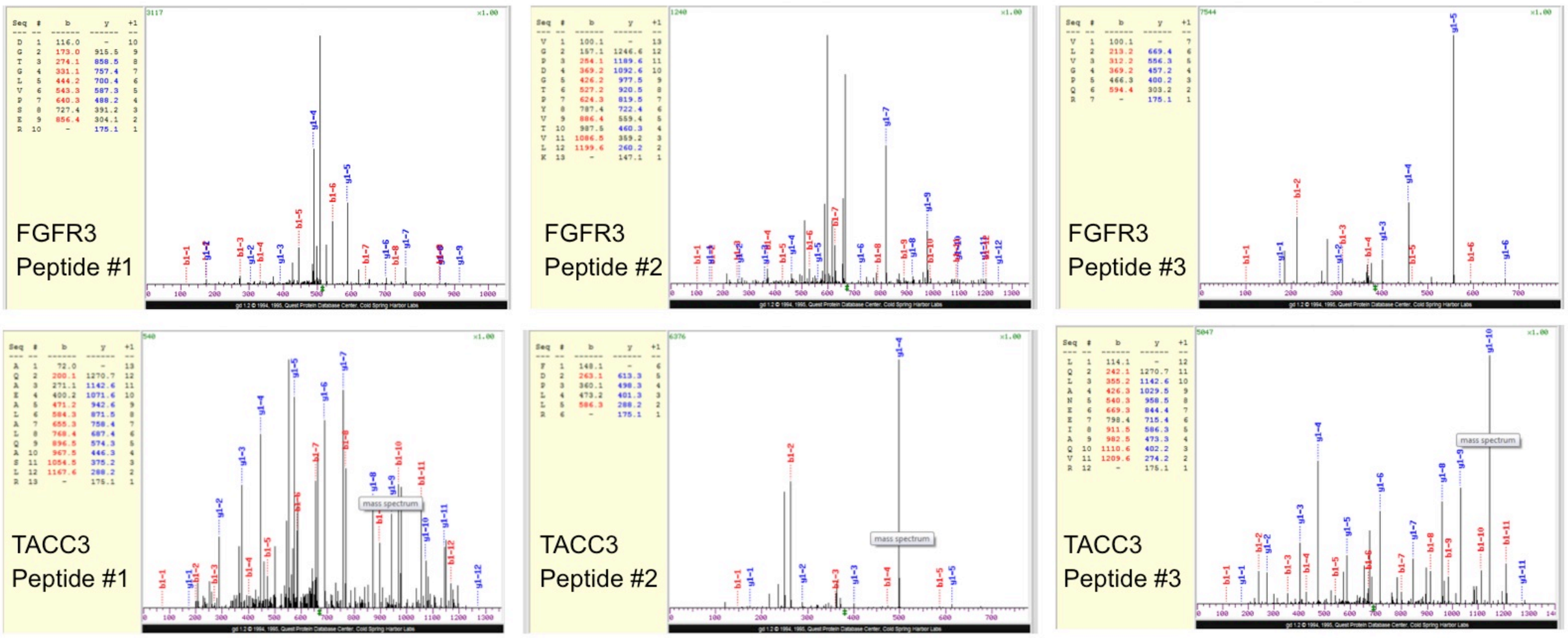

Figure S2

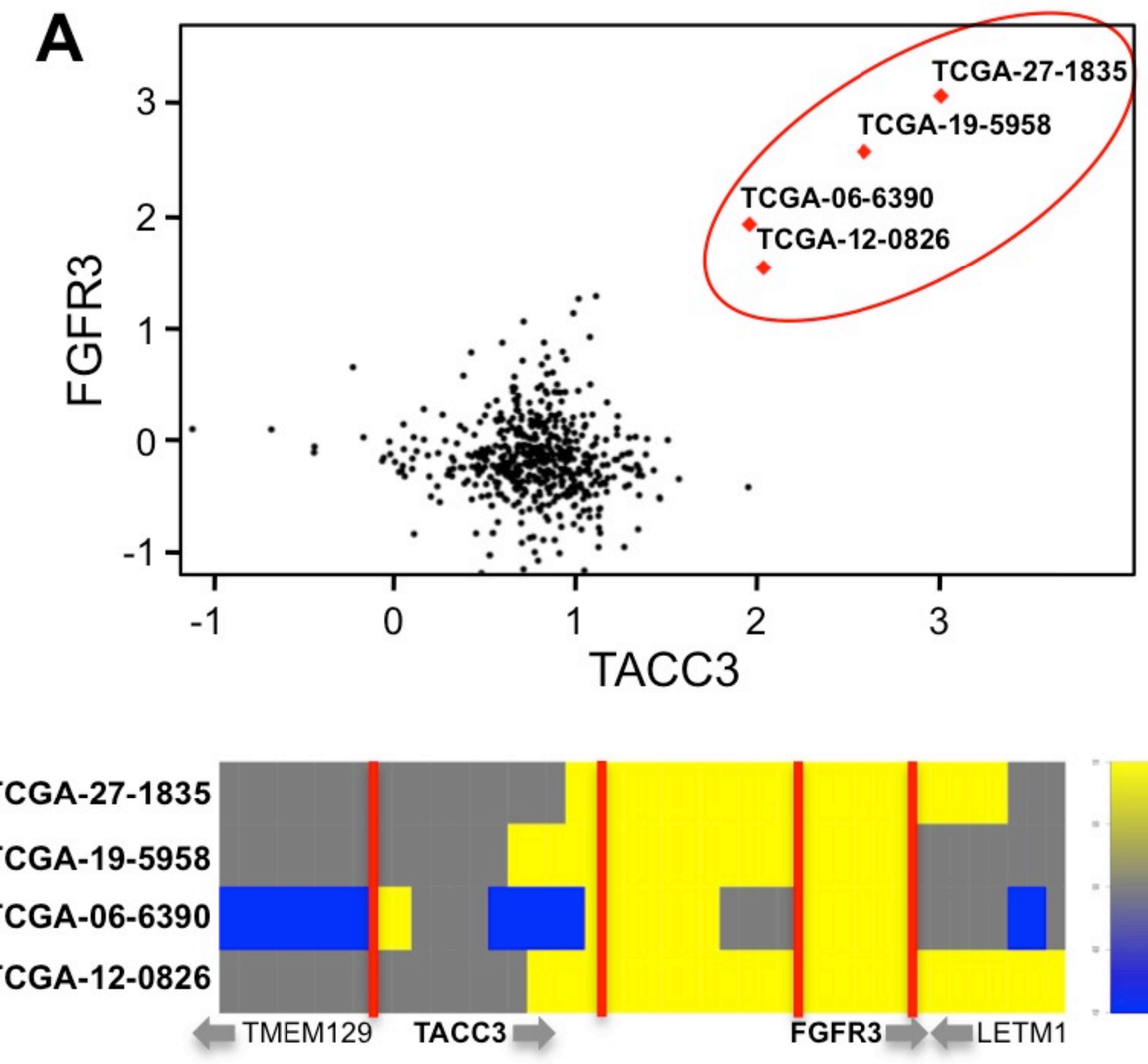
A
TCGA-27-1835
TCGA-19-5958
TCGA-06-6390
TCGA-12-0826
FGFR3
TACC3
3
2
1
0
-1
-1
0
1
2
3
B
TCGA-27-1835
TCGA-19-5958
TCGA-06-6390
TCGA-12-0826
TMEM129
TACC3
FGFR3
LETM1

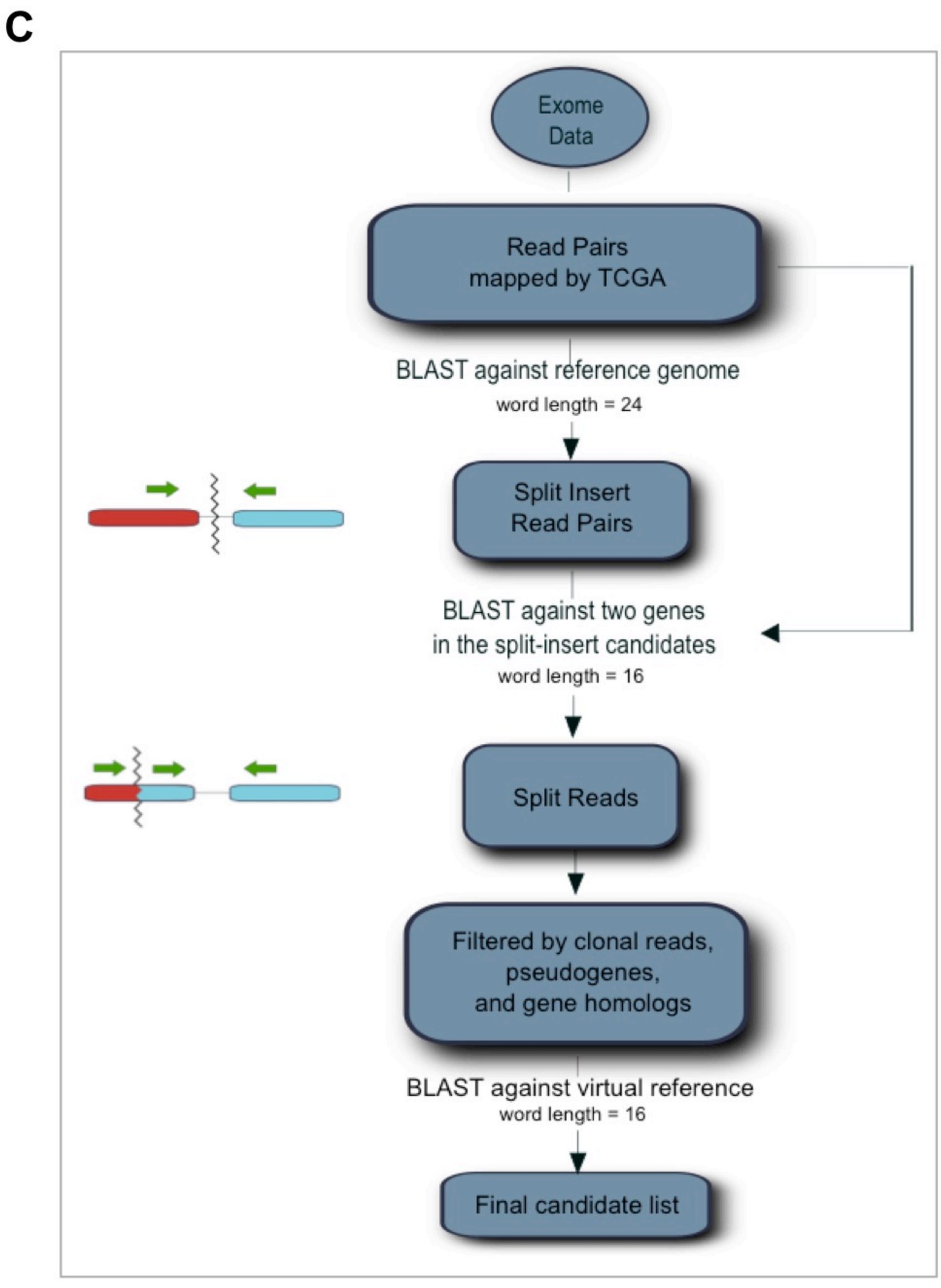
C
Exome Data
Read Pairs mapped by TCGA
BLAST against reference genome
word length = 24
Split Insert Read Pairs
BLAST against two genes in the split-insert candidates
word length = 16
Split Reads
Filtered by clonal reads, pseudogenes, and gene homologs
BLAST against virtual reference
word length = 16
Final candidate list

Figure S3

A

TCGA-27-1835

5'	FGFR3: Intron 16	1778595	1709397	TACC3: Intron 10	3'
	CATCCTGCCCCCCAGAGTGCTGAGGTGTGGGGCGGGCCTTCTGGGGCACAGCCTGGGCACAGAGGTGGCTGTGCGA		AGGTCGCTGAGGGTCCAGGCTTCCACCCAGTGTCCCCGCAGTCAGCTGCCCACCAGCAGCCTCCCCGGGACTCTCC		
R	GGCTGGGCGA		AGTTCGCTGAGGGTCCAGGCTTCCTCCCAGTGTCCCCGCAGTCAGCTGCCCACCAGCAGCCTCCCC		
F	ACAGCCTGGGCACAGAGGTGGCTGTGCGA		AGGTCGCTGAGGGTCCAGGCTTCCACCCAGTGTCCCCGCAGTCAGCT		
R	GGCACAGCCTGGGCACAGAGGTGGCTGTGCGA		AGGTCGCTGAGGGTCCAGGCTTCCACCCAGTGTCCCCGCAGTCA		
R	TTCTGGGGCACAGCCTGGGCACAGAGGTGGCTGTGCGA		AGGTCGCTGAGGGTCCAGGCTTCCACCCAGTGTCCCCG		
R	CTTCTGTGGCACAGCCTGGCCACAGAGGTGGCTGTGCGA		AGGTCGCTGAGGGTCCAGGCTTCCACCCAGTGTCCCC		
R	GCCTTCTGGGGCACAGCCTGGGCACAGAGGTGGCTGTGCGA		AGGTCGCTGAGGGTCCAGGCTTCCACCCAGTGTCC		
R	GGTGTGGGGCGGGCCGGCTGGGGCACAGCCGGGGCACAGAGGTGGCTGTGCGA		AGGTCGCTGAGGGTCCAGGCTTC		
R	GGTGTGGGGCGGGCCTTCTGGGGCACAGCCTGGGCACAGAGGTGGCTGTGCGA		AGGTCGCTGAGGGTCCAGGCTTC		
R	TGCTGAGGTGTGGGGCGGGCCTTCTGGGGCACAGCCTGGGCACAGAGGTGGCTGTGCGA		AGGTCGCTGAGGGTCCA		
R	AGTGCTGAGGTGTGGGGCGGGCCTTCTGGGGCACAGCCTGGGCACAGAGGTGGCTGTGCGA		AGGTCGCTGAGGGTC		
R	CCCAGAGTGCTGAGGTGTGGGGCGGGCCTTCTGGGGCACAGCCTGGGCACAGAGGTGGCTGTGCGA		AGGTCGCTGA		
R	CCTGCCCCCCAGAGTGCTGAGGTGTGGGGCGGGCCTTCTGGGGCACAGCCTGGGCACAGAGGTGGCTGTGCGA		AGG		

TCGA-19-5958

5'	FGFR3: Intron 16	1778539	1707202	TACC3: Intron 7	3
	GTGCTGGCTCTGGCCTGGTGCCACCCGCCTATGCCCCTCCCCCTGCCGTCCCCGGCCATCCTGCCCCCCAGAGTGC		CGGGGGCTAAGGGCCAGGGAGGTCACCTGCACACTCCCACCCCCGGTCACCCGCACACTCCCACCCCCGGTCACCCA		
R	AGAGTGC		AGGGGGCTAAGGGCCAGGGAGGTCACCTGCACACTCCCACCCCCGGTCACCCGCACACTCCCACCCCCG		
R	GGCCATCCTGCCCCCCAGAGTGC		AGGGGGCTAAGGGCCAGGGAGGTCCCCTGCACACTCCCTCCCCCGGTCACCCG		
R	TCCCCCTGCCGTCCCCGGCCATCCTGCCCCCCAGAGTGC		AGGGGGCTAAGGGCCAGGGAGGTCACCTGCACACTCC		

TCGA-06-6390

5'	FGFR3: Intron 16	1778521	1708787	TACC3: Exon 9	3'
	TGACGTCCACCGACGTGAGTGCTGGCTCTGGCCTGGTGCCACCCGCCTATGCCCCTCCCCCTGCCGTCCCCGGCCA		TCCCTCAGGACGTCCGCGGGAAGCCAAGCTTGTGGAGTTCGATTTCTTGGGAGCACTGGACATTCCTGTAAGTCCT		
R	A		TCCCTCAGGACGTCCGCGGGAAGCCAAGCTTGTGGAGTTCGATTTCTTGGGAGCACTGGACATTCCTGTAAGTCC		
F	CA		TCCCTCAGGACGTCCGCGGGAAGCCAAGCTTGTGGAGTTCGATTTCTTGGGAGCACTGGACATTCCTGTAAGTC		
F	CA		TCCCTCAGGACGTCCGCGGGAAGCCAAGCTTGTGGAGTTCGATTTCTTGGGAGCACTGGACATTCCTGTAAGTC		
F	GCCA		TCCCTCAGGACGTCCGCGGGAAGCCAAGCTTGTGGAGTTCGATTTCTTGGGAGCACTGGACATTCCTGTAAG		
F	CCGGCCA		TCCCTCAGGACGTCCGCGGGAAGCCAAGCTTGTGGAGTTCGATTTCTTGGGAGCACTGGACATTCCTGT		
R	CACGGCCA		TCCCGGAGGACGTCCGCGGGAACCCAAGCTTGTGGAGTTCGATTTCTTGGTAGCACTGGACATTCCTG		
R	CCCGGCCA		TCCCTCAGGACGTCCGCGGGAAGCCAAGCTTGTGGAGTTCGATTTCTTGGGAGCACTGGACATTCCTG		
F	TCCCCGGCCA		TCCCTCAGGACGTCCGCGGGAAGCCAAGCTTGTGGAGTTCGATTTCTTGGGAGCACTGGACATTCC		
F	TCCCCGGCCA		TCCCTCAGGANGTCCGCGGGAAGCCAAGCTTGTGGAGTTCGATTTCTTGGGAGCACTGGACATTCC		
F	GTCCCCGGCCA		TCCCTCAGGACGTCCGCGGGAAGCCAAGCTTGTGGAGTTCGATTTCTTGGGAGCACTGGACATTC		
F	CCGTCCCCGGCCA		TCCCTCAGGACGTCCGCGGGAAGCCAAGCTTGTGGAGTTCGATTTCTTGGGAGCACTGGACAT		
R	TCCCCCTGCCGTCCCCGGCCA		TCCCTCAGGACGTCCGCGGGAAGCCAAGCTTGTGGAGTTCGATTTCTTGGGAGCA		
R	ATGCCCCTCCCCCTGCCGTCCCCGGCCA		TCCCTCAGGACGTCCGCGGGAAGCCAAGCTTGTGGAGTTCGATTTCTT		
R	CCTATGCCCCTCCCCCTGCCGCCCCCGGCCA		TCCCTCAGGACGTCCGCGGGAAGCCAAGCTTGTGGAGTTCGATTT		
F	CTGGCCTGGTGCCACCCGCCTATGCCCCTCCCCCTGCCGTCCCCGGCCA		TCCCTCAGGACGTCCGCGGGAAGCCAA		
R	GAGCTGGCCTGGTGCCACACGCCTATGCCCCTCCCCCTGCCGTCCCCGGCGA		TCCATCAGGAAGTCCGCGGGACGA		
R	GGCTCTGGCCTGGTGCCACCCGCCTATGCCCCTCCCCCTNCCGTCCCCGGCCA		TCCCTCAGGACGTCCGCGGGAAG		
F	GTGCTGGCTCTGGCCTGGTGCCACCCGCCTATGCCCCTCCCCCTGCCGTCCCCGGCCA		TCCCTCAGGACGTCCGCG		
R	CCACCGACGTGAGTGCTGGCTCTGGCCTGGTGCCACCCGCCTATGCCCCTCCCCCTGCCGTCCCCGGCCA		TCCCTC		

TCGA-12-0826

5'	FGFR3: Intron 16	1778502	1707185	TACC3: Intron 7	3'
	CTGGACCGTGTCCTTACCGTGACGTCCACCGACGTGAGTGCTGGCTCTGGCCTGGTGCCACCCGCCTATGCCCCTC		CCCTGGCCCTTAG-CCCCC-GTGTGTGTTAGGGGATGGCAGTCAGACCTGATCACTTGCCCTCTTGTCCCAGTTTAA		
R	TGCCCCTC		CCCT-GCCCTTAGCCCCCCTGTGTGTGTTAGGGGATGGCAGTCAGACCTGATCACTTGCCCTCTTGTCC		
F	ATGCCCCTC		CCCT-GCCCTTAGCCCCCCTGTGTGTGTTAGGGGATGGCAGTCAGACCTGATCACTTGCCCTCTTGTC		
F	GCCTATGCCCCTC		CCCT-GCCCTTAGCCCCCCTGTGTGTGTTAGGGGATGGCAGTCAGACCTGATCACTTGCCCTCT		
F	GTGCCACCCGCCTATGCCCCTC		CCCT-GCCCTTAGCCCCCCTGTGTGTGTTAGGGGATGGCAGTCAGACCTGATCAC		
R	GCTCTGGCCTGGTGCCCCCCGCCTATGCCCCTC		CCCT-GCCCTTAGCCCCCCTGTGTGTGTTAGGGGATGGCAGTCA		
R	GCTCTGGCCTGGTGCCCCCCGCCTATGCCCCTC		CCCT-GCCCTTAGCCCCCCTGTGTGTGTTAGGGGATGGCAGTCA		
R	GCTGCCTCTGTCCTGGTGCCCCCCGCCTATGCCCCTC		CCCT-GCCCTTAGCCCCCCTGTGTGTGTTAGGGGATGGCA		
R	CCCCCCGACGTGAGTGCTGGCTCGGGCCTGGTCCCCCCCGCCTATGCCCCTC		CCCT-GCCCTTAGCCCCCCTGTGTG		
F	GACGTCCACCGACGTGAGTGCTGGCTCTGGCCTGGTGCCACCCGCCTATGCCCCTC		CCCT-GCCCTTAGACCCCCTG		
F	CTTACCGTGACGTCCACCGACGTGAGTGCTGGCTCTGGCCTGGTGCCACCCGCCTATGCCCCTC		CCCT-GCCCTTAG		
F	TGTCCTTACCGTGACGTCCACCGACGTGAGTGCTGGCTCTGGCCTGGTGCCACCCGCCTATGCCCCTC		CCCT-GCCC		

B

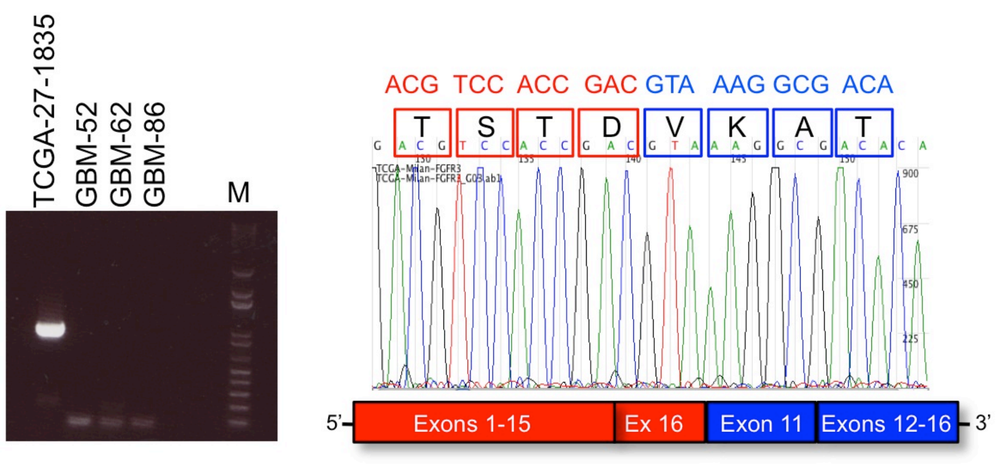

C

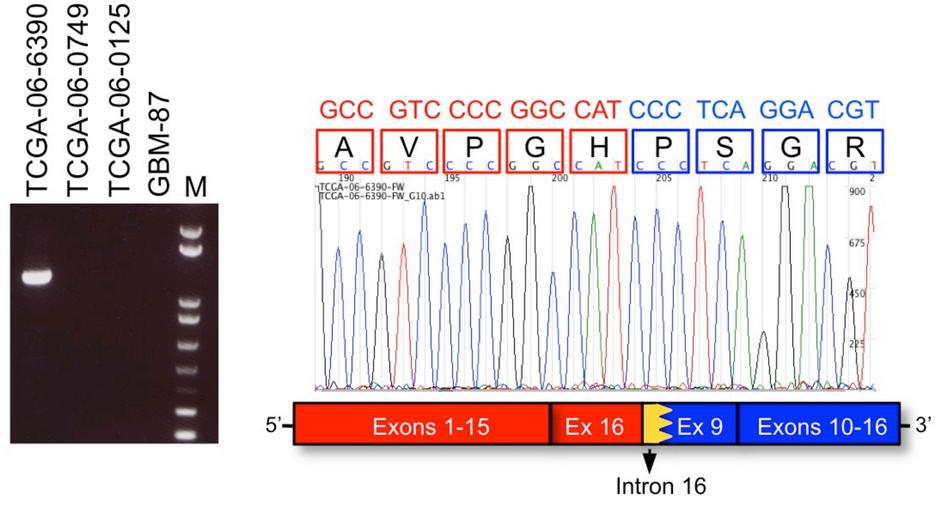

D

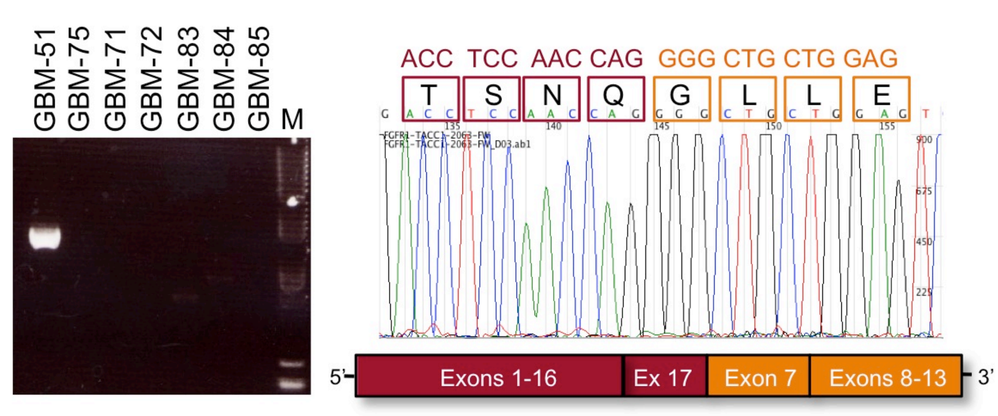

E

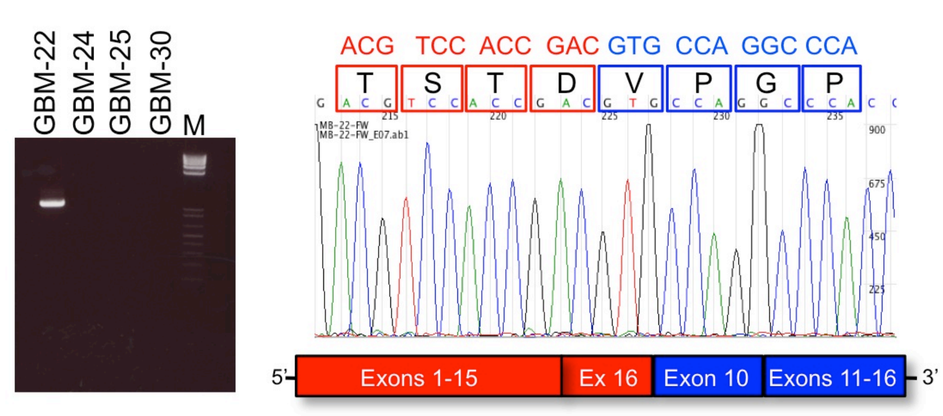

Figure S4

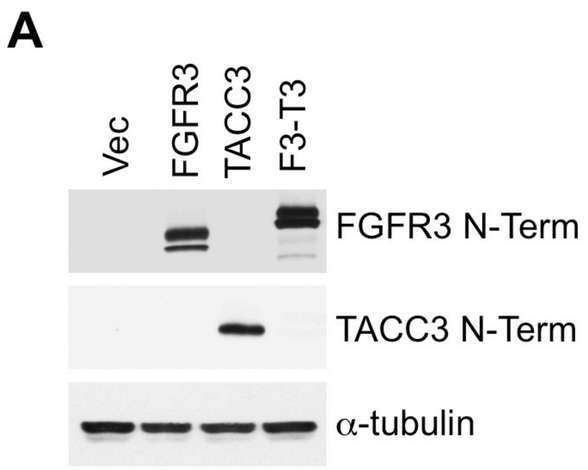
A
Vec
FGFR3
TACC3
F3-T3
FGFR3 N-Term
TACC3 N-Term
α-tubulin

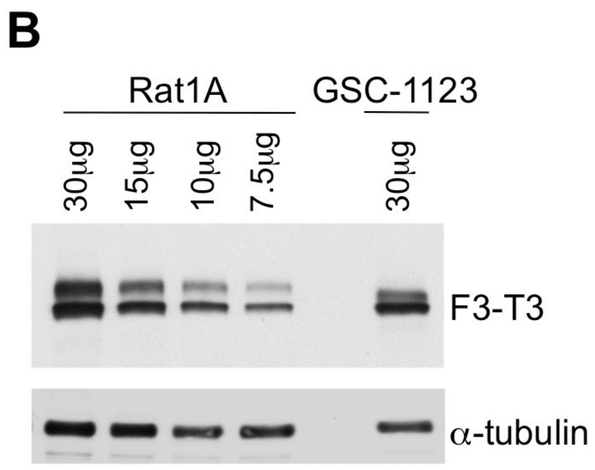
B
Rat1A
GSC-1123
30μg
15μg
10μg
7.5μg
30μg
F3-T3
α-tubulin

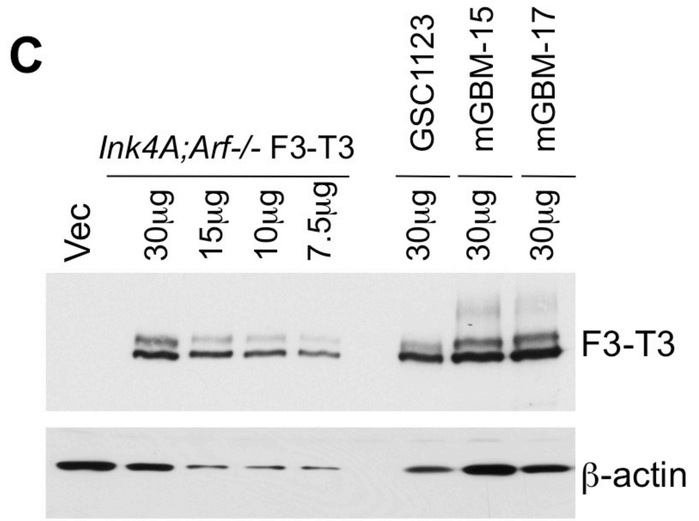
C
Ink4A;Arf-/- F3-T3
GSC1123
mGBM-15
mGBM-17
Vec
30μg
15μg
10μg
7.5μg
30μg
30μg
30μg
F3-T3
β-actin

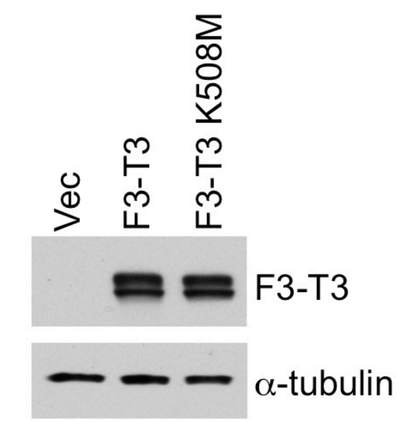
D
Vec
F3-T3
F3-T3 K508M
F3-T3
α-tubulin

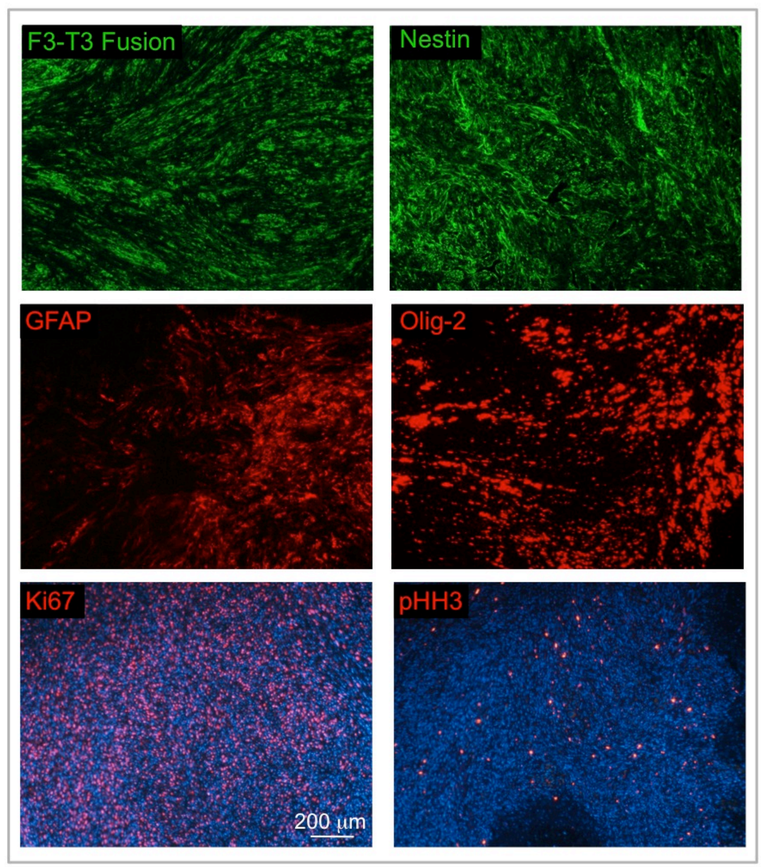
E
F3-T3 Fusion
Nestin
GFAP
Olig-2
Ki67
pHH3
200 μm

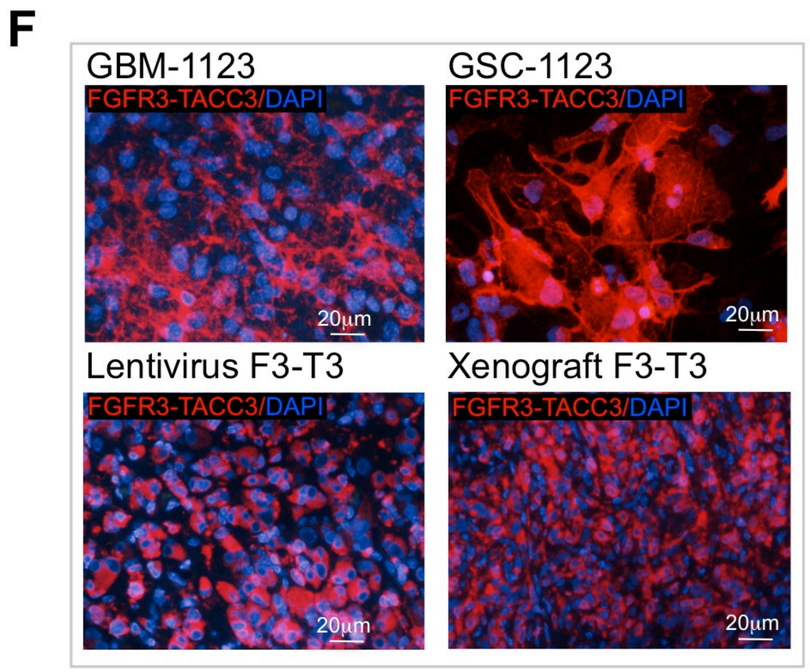
F
GBM-1123
FGFR3-TACC3/DAPI
GSC-1123
FGFR3-TACC3/DAPI
20μm
Lentivirus F3-T3
FGFR3-TACC3/DAPI
Xenograft F3-T3
FGFR3-TACC3/DAPI
20μm

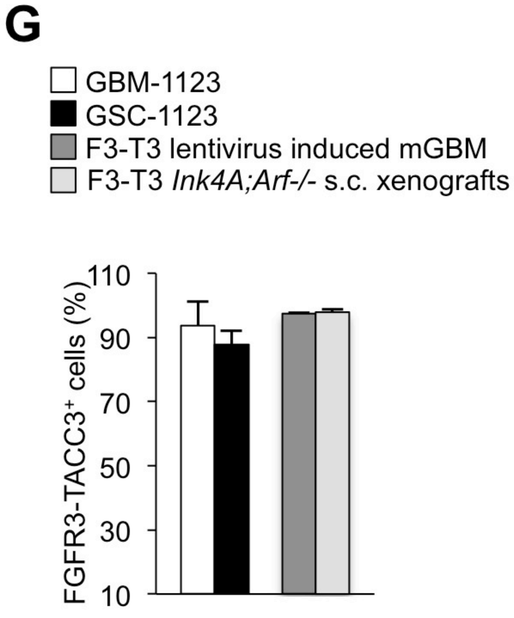
G
GBM-1123
GSC-1123
F3-T3 lentivirus induced mGBM
F3-T3 Ink4A;Arf-/- s.c. xenografts
FGFR3-TACC3+ cells (%)
110
90
70
50
30
10

Figure S5

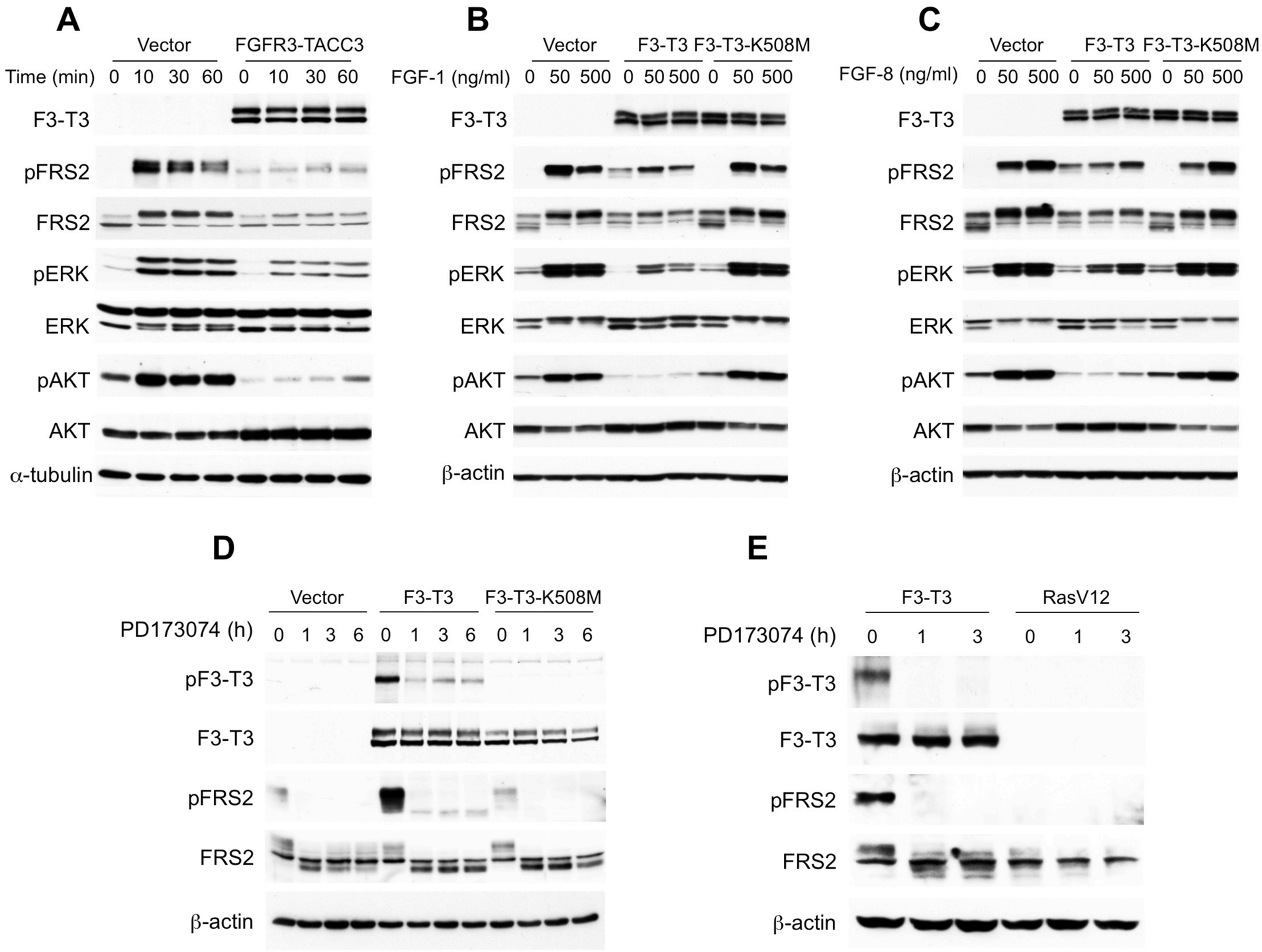
A
Vector
FGFR3-TACC3
Time (min) 0 10 30 60 0 10 30 60
F3-T3
pFRS2
FRS2
pERK
ERK
pAKT
AKT
α-tubulin
B
Vector
F3-T3
F3-T3-K508M
FGF-1 (ng/ml) 0 50 500 0 50 500 0 50 500
F3-T3
pFRS2
FRS2
pERK
ERK
pAKT
AKT
β-actin
C
Vector
F3-T3
F3-T3-K508M
FGF-8 (ng/ml) 0 50 500 0 50 500 0 50 500
F3-T3
pFRS2
FRS2
pERK
ERK
pAKT
AKT
β-actin
D
Vector
F3-T3
F3-T3-K508M
PD173074 (h) 0 1 3 6 0 1 3 6 0 1 3 6
pF3-T3
F3-T3
pFRS2
FRS2
β-actin
E
F3-T3
RasV12
PD173074 (h) 0 1 3 0 1 3
pF3-T3
F3-T3
pFRS2
FRS2
β-actin

Figure S6

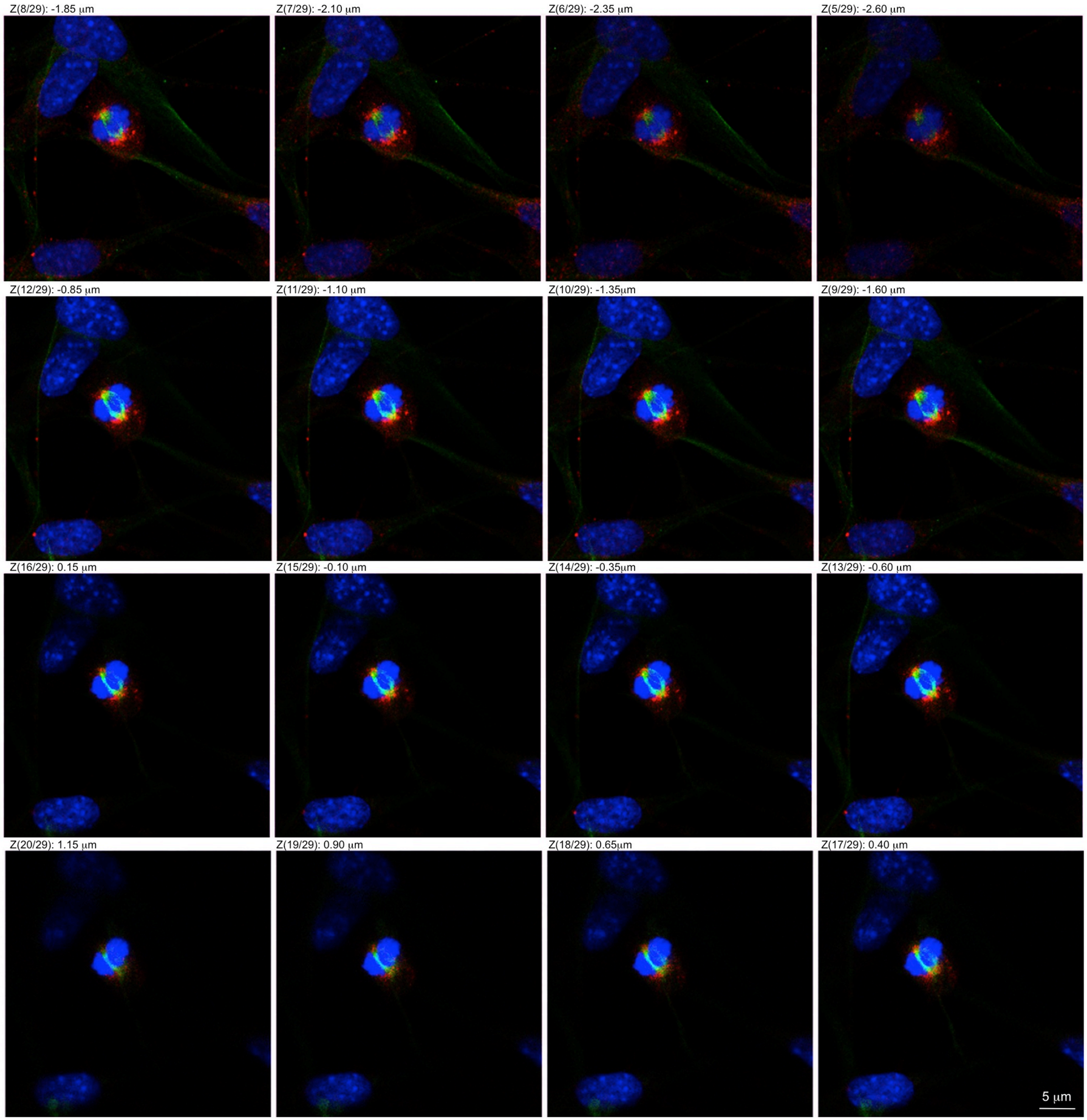
Z(8/29): -1.85 μm
Z(7/29): -2.10 μm
Z(6/29): -2.35 μm
Z(5/29): -2.60 μm
Z(12/29): -0.85 μm
Z(11/29): -1.10 μm
Z(10/29): -1.35μm
Z(9/29): -1.60 μm
Z(16/29): 0.15 μm
Z(15/29): -0.10 μm
Z(14/29): -0.35μm
Z(13/29): -0.60 μm
Z(20/29): 1.15 μm
Z(19/29): 0.90 μm
Z(18/29): 0.65μm
Z(17/29): 0.40 μm
5 μm

Figure S7

A

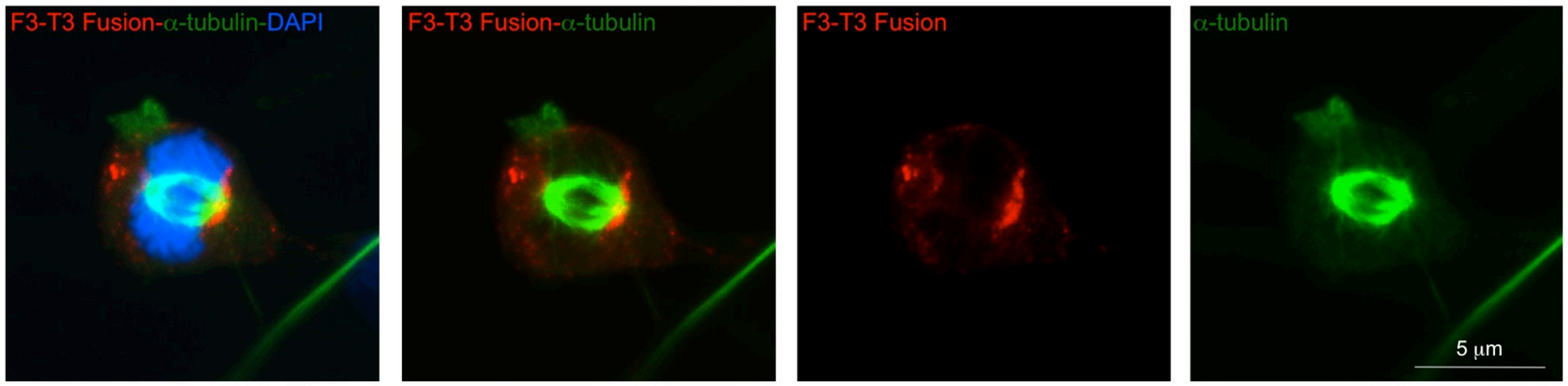

B

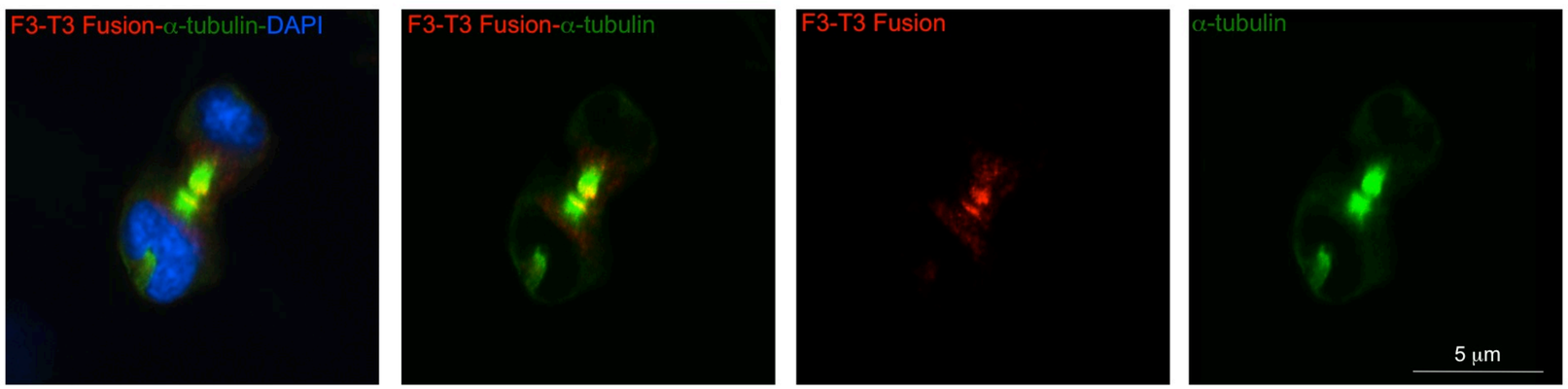

C

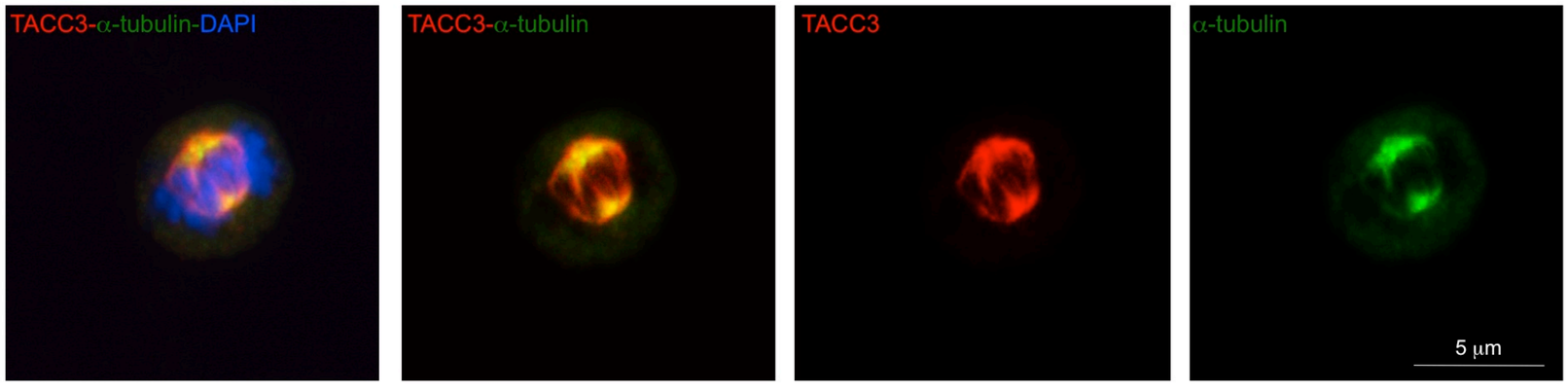

D

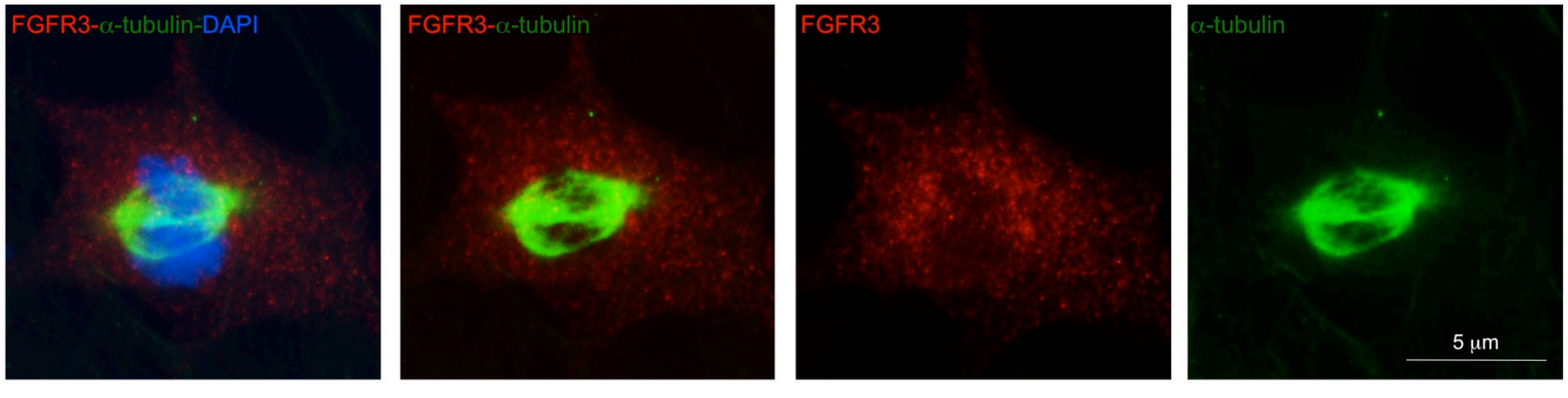

Figure S8

A

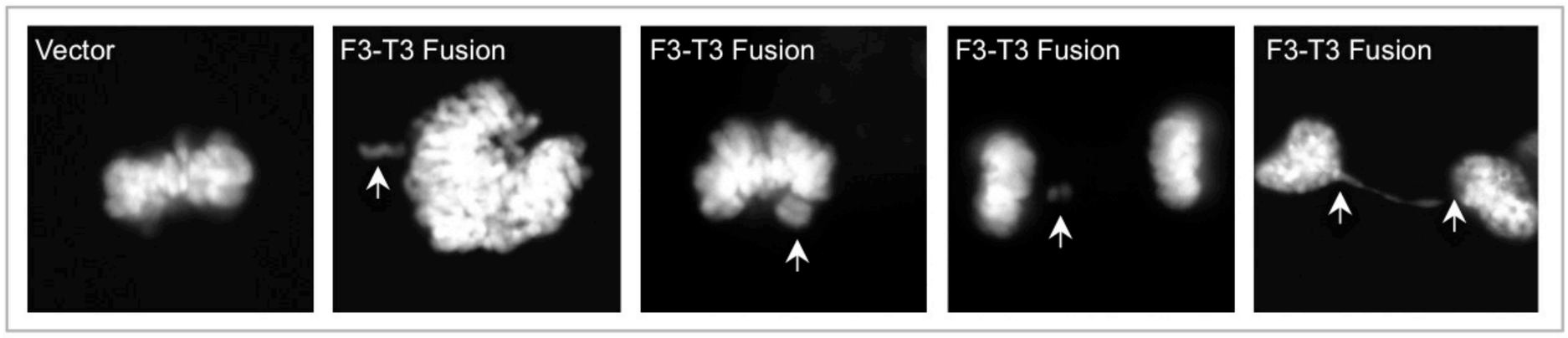

B

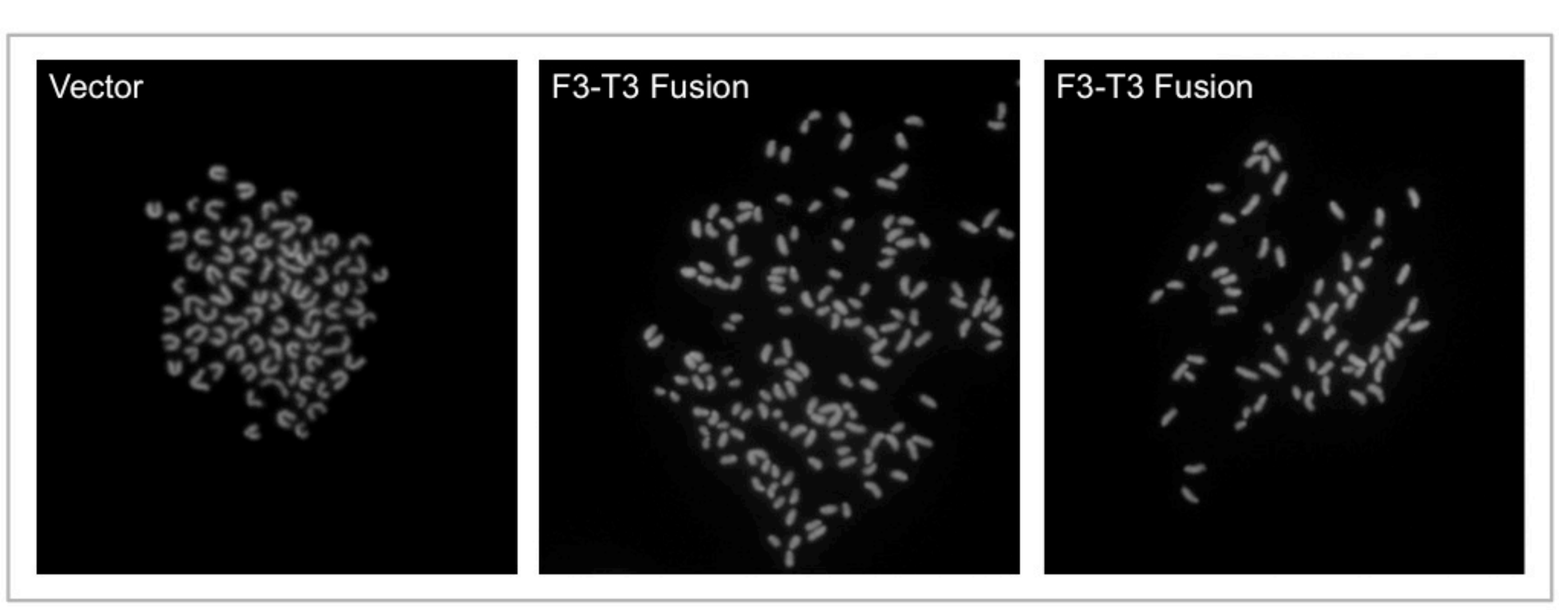

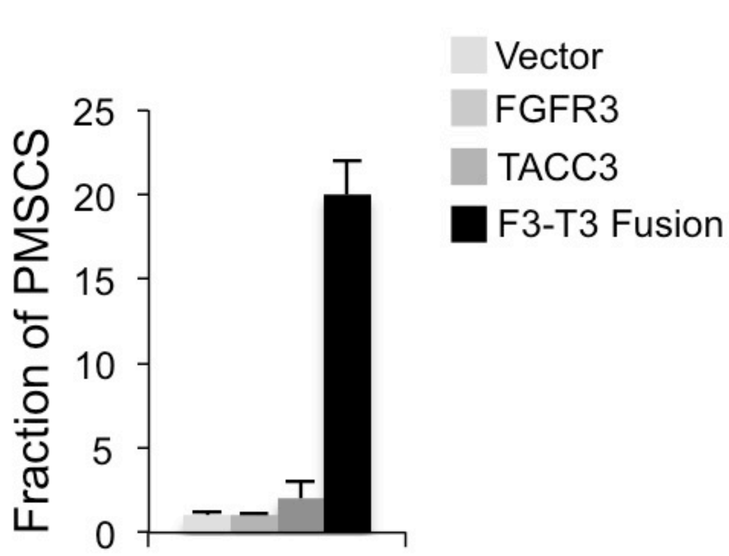

C

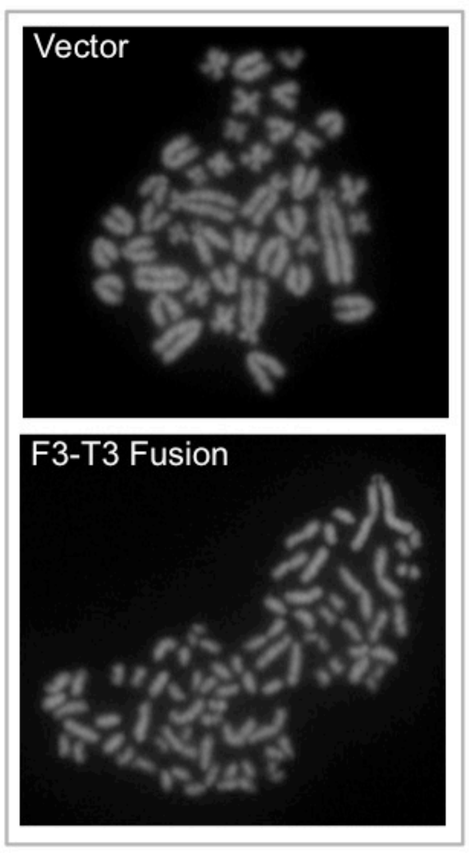

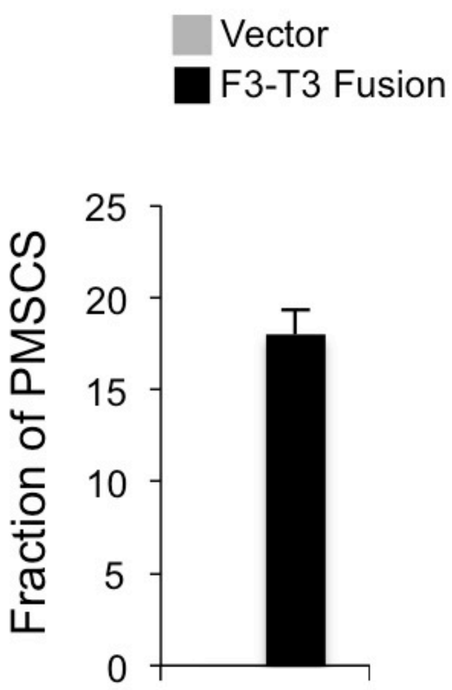

D

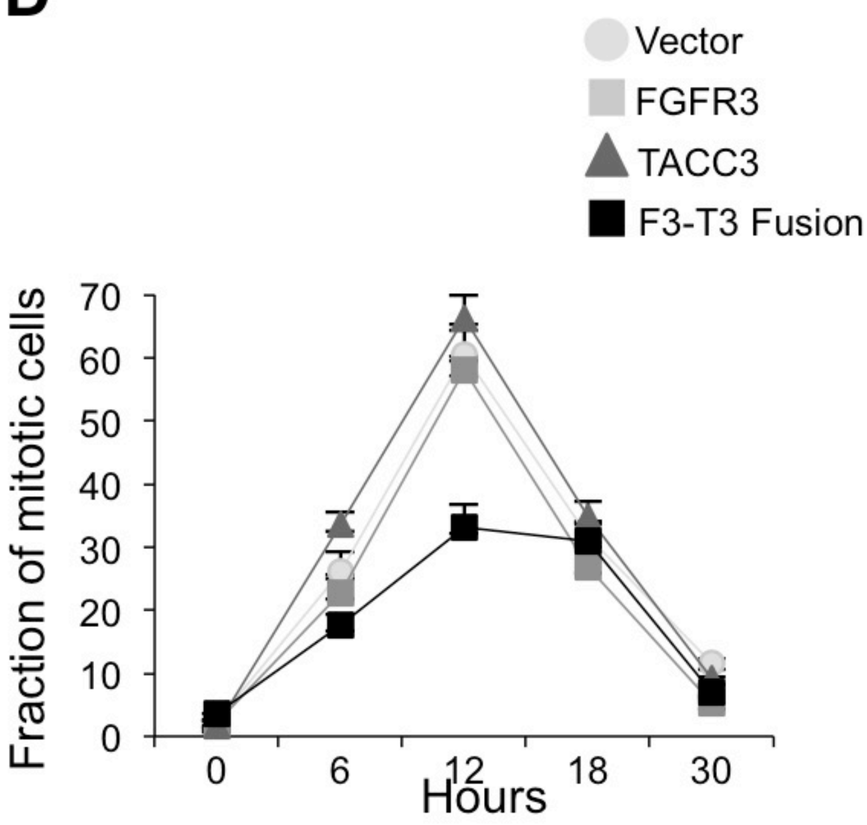

E

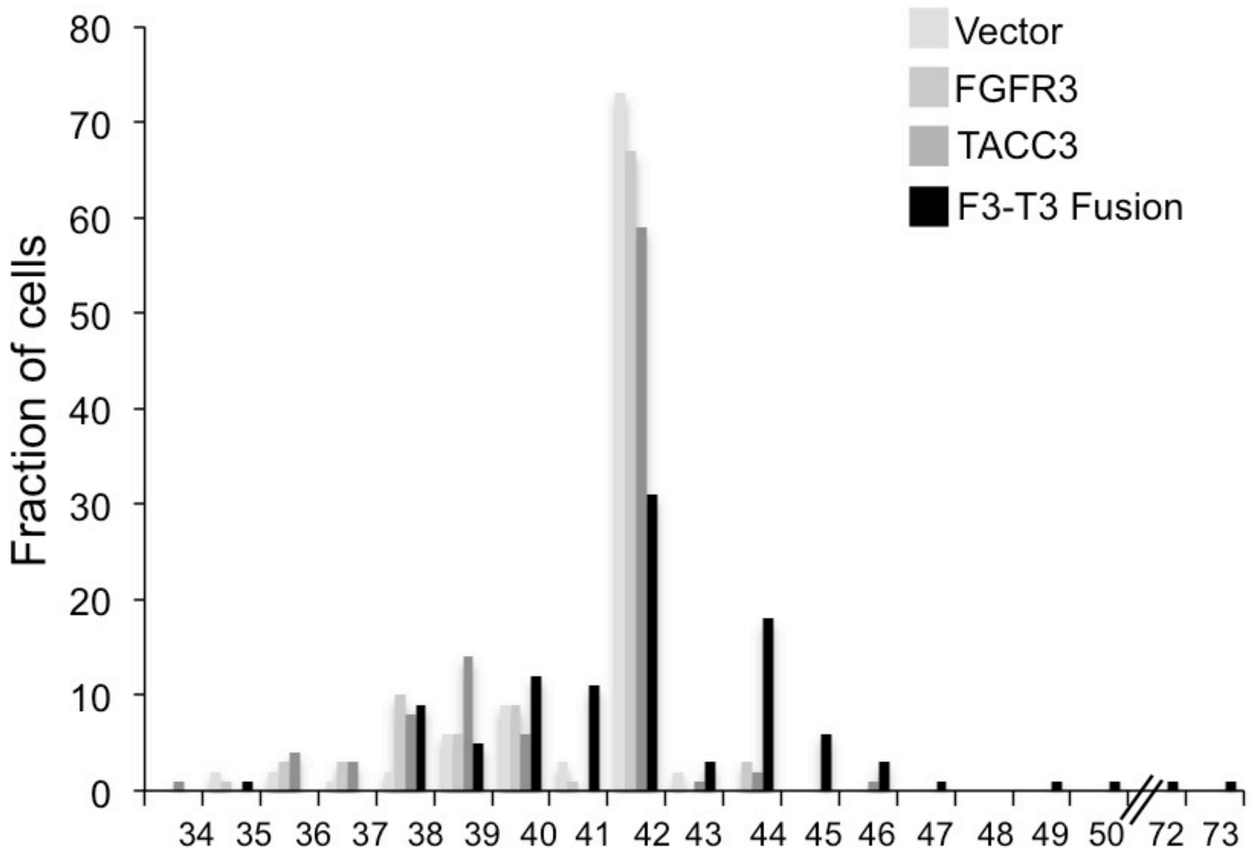

F

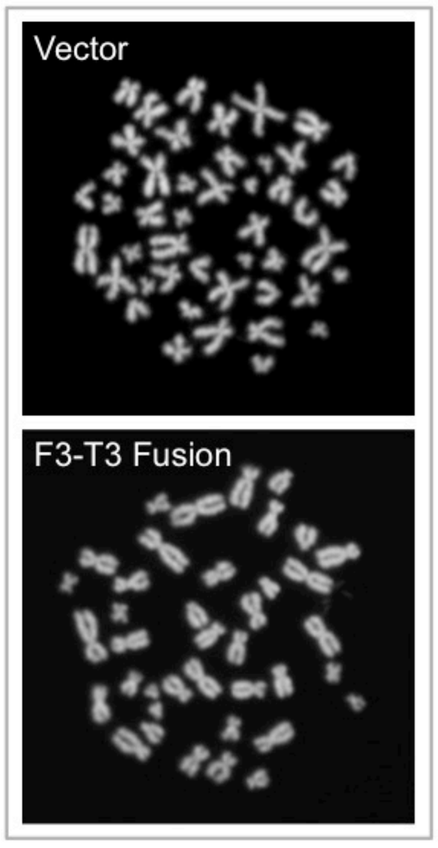

Figure S9

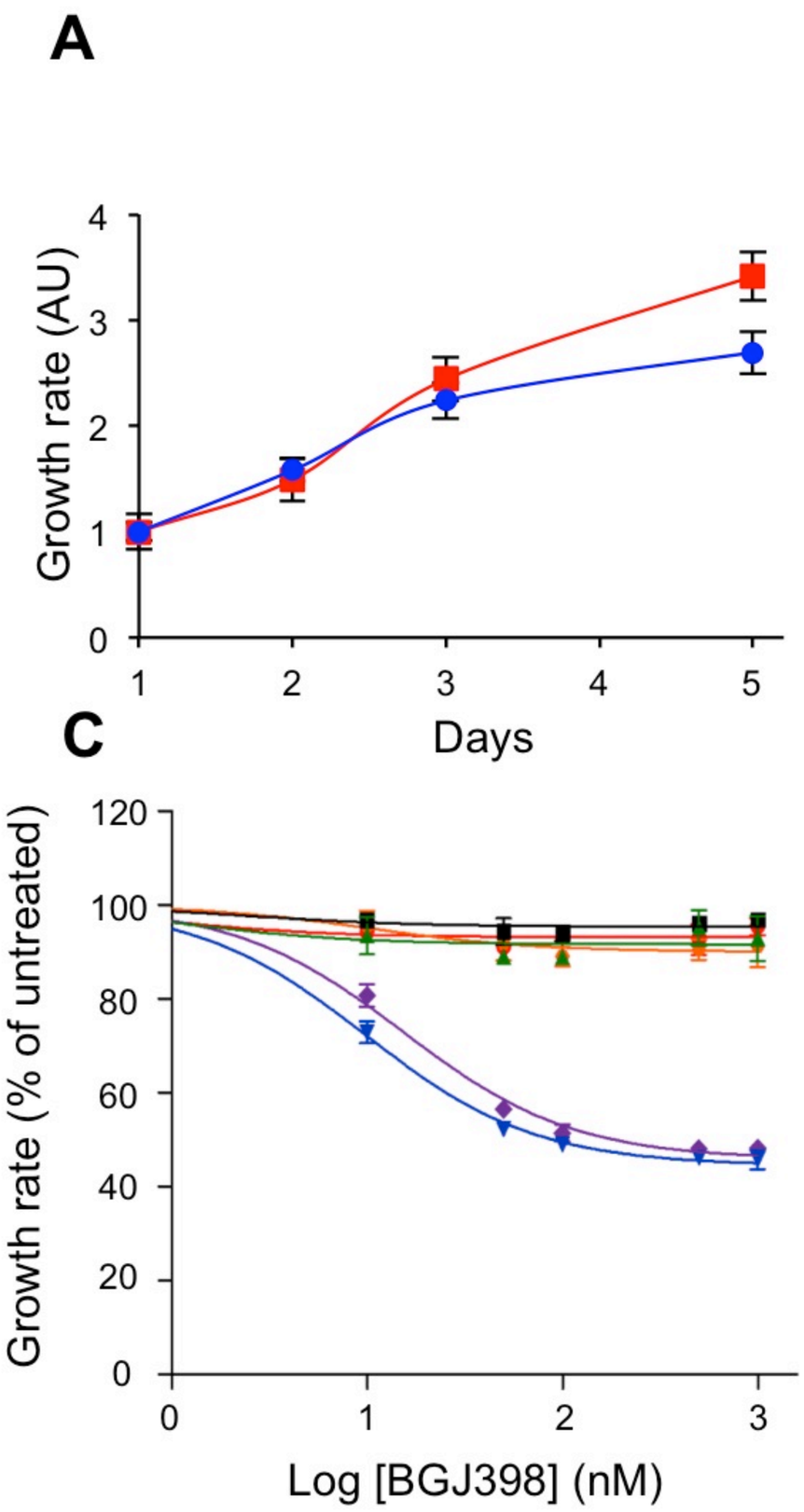
A
Growth rate (AU)
Days
B
Vec
F3-T3
C
Growth rate (% of untreated)
Log [BGJ398] (nM)
D
Log [AZD4547] (nM)
Vec
FGFR3
TACC3
F3-T3
F3-T3-K508M
F1-T1
E
Vec
F3-T3
sh-Ctr sh-2 sh-3 sh-4
F3-T3
β-actin
Growth rate (AU)
Days
Vec
sh-Ctr
sh-2
sh-3
sh-4
F
sh-Ctr sh-3 sh-4
F3-T3
β-actin
Number of cells (X10³)
Days
sh-Ctr
sh-3
sh-4
G
Tumor Volume (mm³)
Days
Control
PD173074

Figure S10

Table S1. Predicted in-frame fusion proteins from RNA-Seq of nine GSCs

Sample	#SplitInserts	#SplitReads	Gene1	Gene2	RefSeq1	RefSeq2	TxPos1	TxPos2	Chr1	Strand1	hg19_GenPos1	Chr2	Strand2	hg19_GenPos2
GSC-1123	294	76	FGFR3	TACC3	NM_000142	NM_006342	2530	1751	4	+	1808842	4	+	1737004
GSC-0114	37	54	POLR2A	WRAP53	NM_000937	NM_001143990	479	798	17	+	7399259	17	+	7604059
GSC-0114	7	48	CAPZB	UBR4	NM_001206540	NM_020765	228	12111	1	-	19712098	1	-	19433440
GSC-0517	8	29	ST8SIA4	PAM	NM_005668	NM_000919	1125	730	5	-	100147809	5	+	102260661
GSC-0308	6	17	PIGU	NCOA6	NM_080476	NM_014071	729	6471	20	-	33203914	20	-	33303130
GSC-0127	1	6	IFNAR2	IL10RB	NM_000874	NM_000628	1083	149	21	+	34632901	21	+	34640699

Table S2. List of split inserts supporting the identification of FGFR3-TACC3 fusion genes in four GBM samples from the TCGA exome collection

TCGAsampleID	gene1	gene1 length	readID	%identity	length	mismatch	gap	read start	read end	hg18 genome	hg18 genome	e-value	bit score	read 1 fasta
TCGA-06-6390	FGFR3	76	C01PRACXX110628:1:1301:1934:116558	100	76	0	0	1	76	1778372	1778447	8E-40	151	GTGCTGGCATGCCGCGCCCTCCCAGAGGCCCACCTTCAAGCAGCTGGTGGAGGACCTGGACCGTGTCCTTACCGTG
TCGA-06-6390	FGFR3	76	C01RDACXX110628:3:2305:4872:47008	98.68	76	1	0	1	76	1778364	1778439	2E-37	143	ATGCGGGAGTGCTGGCATGACGCGCCCTCCCAGAGGCCCACCTTCAAGCAGCTGGTGGAGGACCTGGACCGTGTCC
TCGA-06-6390	FGFR3	76	D03U9ACXX110625:6:1203:16178:138219	100	76	0	0	1	76	1778413	1778488	8E-40	151	AGCTGGTGGAGGACCTGGACCGTGTCCTTACCGTGACGTCCACCGACGTGAGTGCTGGCTCTGGCCTGGTGCCACC
TCGA-06-6390	TACC3	76	C01PRACXX110628:2:1102:13552:120312	100	76	0	0	1	76	1708918	1708843	8E-40	151	CCCTTAAAACAACTCGTTCCCTCAGACCACACACAAGACAGTTCAAGAGGGACTCAAGGACTTACAGGAATGTCCA
TCGA-06-6390	TACC3	76	C01PRACXX110628:8:2308:6515:60354	100	76	0	0	1	76	1708956	1708881	8E-40	151	AACCAAAGGCTCAGACCCCCAGGAATAGAAAATATAGGCCCTTAAAACAACTCGTTCCCTCAGACCACACACAAAGA
TCGA-06-6390	TACC3	76	C01RDACXX110628:6:1305:16843:57213	98.68	76	1	0	1	76	1708865	1708790	2E-37	143	TCAAGGACTTACAGGAATGTCCAGTGCTCCCAAGAAATCGAACTCCACAAGCTTGGCTTCCCGCGCACGTCCTGAG
TCGA-06-6390	TACC3	75	D03U9ACXX110625:2:1202:19578:90281	100	75	0	0	1	75	1708861	1708787	3E-39	149	GGACTTACAGGAATGTCCAGTGCTCCCAAGAAATCGAACTCCACAAGCTTGGCTTCCCGCGGACGTCCTGAGGGAT
TCGA-06-6390	TACC3	76	D03U9ACXX110625:4:2306:2694:174970	100	76	0	0	1	76	1708896	1708821	8E-40	151	CAGACCACACACAAGACAGTTCAAGAGGGACTCAAGGACTTACAGGAATGTCCAGTGCTCCCAAGAAATCGAACTC
TCGA-12-0826	FGFR3	72	61C59AAXX100217:4:21:17613:20886	98.61	72	0	1	1	71	1778439	1778510	2E-34	133	CTTACCGTGACGTCCACCGACGTGAGTGCTGGCTCTGGCCTGGTGCCACCCGCCTATGCCCCTCCCCTGCCCTTAG
TCGA-12-0826	TACC3	75	42MJNAAXX090813:5:30:1412:1280#0	100	75	0	0	2	76	1707299	1707225	3E-39	149	AAACTTGAGGTATAAGGACTGCTTCCTCAAGGCCGACCTCCTTAAACTGGGGACAAGAGGGCAAGTGATCAGGTCTG
TCGA-12-0826	TACC3	76	61C59AAXX100217:4:2:4279:6949	100	76	0	0	1	76	1707299	1707224	8E-40	151	AACTTGAGGTATAAGGACTGCTTCCTCAAGGCCGACTCCTTAAACTGGGGACAAGAGGGCAAGTGATCAGGTCTGA
TCGA-12-0826	FGFR3	76	42MJNAAXX090813:5:37:435:1250#0	100	76	0	0	1	76	1778346	1778421	8E-40	151	GCCCGCAGGTACATGATCATGCGGGAGTGCTGGCATGCCGCGCCCTCCCAGAGGCCCACCTTCAAGCAGCTGGTGG
TCGA-12-0826	FGFR3	51	61C59AAXX100217:5:89:7727:2557	98.04	51	1	0	1	51	1778443	1778493	4E-24	93.7	ACCGTGACGTCCACCGACGTGAGTGCTGGCTCTGGCCTGGTGCGACCCGCCGATCTCTCTCCCCTGTCCTTTTCCT
TCGA-19-5958	TACC3	62	D03U9ACXX110625:4:2206:9451:114168	90.32	62	6	0	1	62	1707141	1707202	4E-17	75.8	TGGGAGGGTGCGGGGGGCCGGGGGGGGGAGTGTGCAGGTGAGCTCCCTGGCCCTTGGCCCCCTGCCCTCTGGGGGG
TCGA-19-5958	TACC3	74	D03U9ACXX110625:1:2204:20064:21192	95.95	74	3	0	1	74	1707097	1707170	5E-33	123	CTGGGAATGGTGGTGTCTCGGGCAGGGTTGTGGGTGACCGGGGGGTGGGAGGGTGCGGGGGACCGGGGGGGGGAGGG
TCGA-27-1835	FGFR3	76	C00HWABXX110325:7:2202:17680:110666	100	76	0	0	1	76	1778338	1778413	8E-40	151	AGCGCCCTGCCCGCAGGTACATGATCATGCGGGAGTGCTGGCATGCCGCGCCCTCCCAGAGGCCCACCTTCAAGCA
TCGA-27-1835	TACC3	76	C00HWABXX110325:7:1104:10731:5183	100	76	0	0	1	76	1709492	1709417	8E-40	151	GCCAACGCCATGCCCAGGCCGGAGAGTCCCGGGGAGGCTGCTGGTGGGCAGCTGACTGCGGGGACACTGGGTGGAA
TCGA-27-1835	TACC3	60	B09V2ABXX110408:2:2201:5811:24541	100	60	0	0	1	60	1709504	1709445	3E-30	119	AGGCCACCAGAGGCCAACGCCATGCCCAGGCCGGAGAGTCCCGGGGAGGCTGCTGGTGGGGAGGCGAACGCGGGGA
TCGA-27-1835	TACC3	61	B097UABXX110405:4:2102:15742:63594	91.8	61	5	0	1	61	1709482	1709422	6E-19	81.8	TGCCCAGGCCGGAGAGTCCCGGGGCGGCTGCTGGGGGGAGCTGACTGGGGGGGCACTGGGGGGGAGACCCGGGCC

Table S2 continuation

TCGAsampleID	gene2	gene2 length	readID	%identity	length	mismatch	gap	read start	read end	hg18 genome start	hg18 genome end	e-value	bit score	read2 fasta
TCGA-06-6390	TACC3	76	C01PRACXX110628:1:1301:1934:116558	100	76	0	0	1	76	1708922	1708847	8E-40	151	TAGGCCCTTAAAACAACTCGTTCCCTCAGACCACAC ACAAGACAGTTCAAGAGGGACTCAAGGACTTACAG GAATG
TCGA-06-6390	TACC3	76	C01RDACXX110628:3:2305:4872:47008	100	76	0	0	1	76	1708867	1708792	8E-40	151	ACTCAAGGACTTACAGGAATGTCCAGTGCTCCCAAG AAATCGAACTCCACAAGCTTGGCTTCCCGCGGACG TCCTG
TCGA-06-6390	TACC3	76	D03U9ACXX110625:6:1203:16178:138219	100	76	0	0	1	76	1708921	1708846	8E-40	151	AGGCCCTTAAAACAACTCGTTCCCTCAGACCACACA CAAGACAGTTCAAGAGGGACTCAAGGACTTACAGG AATGT
TCGA-06-6390	FGFR3	76	C01PRACXX110628:2:1102:13552:120312	100	76	0	0	1	76	1778387	1778462	8E-40	151	GCCCTCCCAGAGGCCCACCTTCAAGCAGCTGGTGG AGGACCTGGACCGTGTCCTTACCGTGACGTCCACC GACGTG
TCGA-06-6390	FGFR3	76	C01PRACXX110628:8:2308:6515:60354	100	76	0	0	1	76	1778382	1778457	8E-40	151	GCCGCGCCCTCCCAGAGGCCCACCTTCAAGCAGCT GGTGGAGGACCTGGACCGTGTCCTTACCGTGACGT CCACCG
TCGA-06-6390	FGFR3	76	C01RDACXX110628:6:1305:16843:57213	96.05	76	3	0	1	76	1778417	1778492	1E-32	127	GGTGGAGGACCTGGACCGTGACCTTACCGGGACG TCCACCGACGGGAGTGCTGGCTCTGGCCTGGTGC CACCCGCC
TCGA-06-6390	FGFR3	76	D03U9ACXX110625:2:1202:19578:90281	100	76	0	0	1	76	1778447	1778522	8E-40	151	GACGTCCACCGACGTGAGTGCTGGCTCTGGCCTG GTGCCACCCGCCTATGCCCCTCCCCCTGCCGTCCC CGGCCAT
TCGA-06-6390	FGFR3	76	D03U9ACXX110625:4:2306:2694:174970	100	76	0	0	1	76	1778435	1778510	8E-40	151	TGTCCTTACCGTGACGTCCACCGACGTGAGTGCTG GCTCTGGCCTGGTGCCACCCGCCTATGCCCCTCCC CCTGCC
TCGA-12-0826	TACC3	72	61C59AAXX100217:4:21:17613:20886	95.83	72	3	0	1	72	1707362	1707291	3E-30	119	TACCTGCTGGTCTCGGTGGCCACGGGCACTGGTCT ACCAGGGCTGTCCCTCCGGAGGGGGTCAAACTTGA GGGATA
TCGA-12-0826	FGFR3	76	42MJNAAXX090813:5:30:1412:1280#0	98.68	76	1	0	1	76	1778427	1778502	2E-37	143	CTGGACCGTGTCCTTACCGTGACGTCCACCGACGT GAGTGCTGGCTCTGGCCTGGTGCCACCCGCCCATG CCCCTC
TCGA-12-0826	FGFR3	76	61C59AAXX100217:4:2:4279:6949	98.68	76	0	1	1	75	1778435	1778510	8E-37	141	TGTCCTTACCGTGACGTCCACCGACGTGAGTGCTG GCTCTGGCCTGGTGCCACCCGCCTATGCCCCTCCC CTGCCC
TCGA-12-0826	TACC3	67	42MJNAAXX090813:5:37:435:1250#0	98.51	67	1	0	1	67	1707635	1707569	5E-32	125	AAAAGATTTAAGTTTAGATCTTTAATATACCTAGAACG GTGGCTGTAACCAGCAAGGCAGGAGCCCTTTGTGT TGG
TCGA-12-0826	TACC3	75	61C59AAXX100217:5:89:7727:2557	97.33	75	2	0	2	76	1707306	1707232	5E-36	133	TGGGTCAAACTTGAGGTATAAGGACTGCTTCCTCAA GGCCGACTCCTTATACTGGGGACAAGAGGGCAAGT GATCA
TCGA-19-5958	FGFR3	76	D03U9ACXX110625:4:2206:9451:114168	98.68	76	1	0	1	76	1778462	1778537	2E-37	143	GAGTGCTGGCTCTGGCCTGGTGCCACCCGCCTATG CCCCTCCCCCTGGCGTCCCCGGCCATCCTGCCCCC CAGAGT
TCGA-19-5958	FGFR3	76	D03U9ACXX110625:1:2204:20064:21192	100	76	0	0	1	76	1778462	1778537	2E-41	151	GAGTGCTGGCTCTGGCCTGGTGCCACCCGCCTATG CCCCTCCCCCTGCCGTCCCCGGCCATCCTGCCCCC CAGAGT
TCGA-27-1835	TACC3	76	C00HWABXX110325:7:2202:17680:110666	96.05	76	3	0	1	76	1709492	1709417	1E-32	127	GCCAACGCCATGCCCAGGCCGGAGAGTCCCGGGG AGGCTGCTGGTGGGGAGCTGACTTCGGGGACACT GGGGGGAA
TCGA-27-1835	FGFR3	76	C00HWABXX110325:7:1104:10731:5183	96.05	76	3	0	1	76	1778363	1778438	1E-32	127	CATGCGGGAGTGCTGGCATGGCGCGCCCTCCCAG CGGCCCACCTTCAAGCAGCTGGTGGGGGACCTGG ACCGTGTC
TCGA-27-1835	FGFR3	76	B09V2ABXX110408:2:2201:5811:24541	100	76	0	0	1	76	1778458	1778533	8E-40	151	ACGTGAGTGCTGGCTCTGGCCTGGTGCCACCCGC CTATGCCCCTCCCCCTGCCGTCCCCGGCCATCCTG CCCCCCA
TCGA-27-1835	FGFR3	76	B097UABXX110405:4:2102:15742:63594	100	76	0	0	1	76	1778388	1778463	8E-40	151	CCCTCCCAGAGGCCCACCTTCAAGCAGCTGGTGGA GGACCTGGACCGTGTCCTTACCGTGACGTCCACCG ACGTGA

Table S3. List of split reads supporting the identification of FGFR3-TACC3 fusion genes in four GBM samples from TCGA exomes

sample	genesplit1	readid	directionsplit	hg18startsplit1	hg18stopsplit1	length1	mismatch1	gap1	seqsplit
TCGA-06-6390	TACC3	D03U9ACXX110625:2:1202:19578:90281	R	1778521	1778521	1	0	0	GGACTTACAGGAATGTCCAGTGCTCCCAAGAAATCGAACTCC ACAAGCTTGGCTTCCCGCGGACGTCCTGAGGGA***T
TCGA-06-6390	FGFR3	C01PRACXX110628:3:1104:10052:66371	F	1778520	1778521	2	0	0	CA***TCCCTCAGGACGTCCGCGGGAAGCCAAGCTTGTGGAG TTCGATTTCTTGGGAGCACTGGACATTCCTGTAAGTC
TCGA-06-6390	FGFR3	C01PRACXX110628:5:1108:3119:22892	F	1778520	1778521	2	0	0	CA***TCCCTCAGGACGTCCGCGGGAAGCCAAGCTTGTGGAG TTCGATTTCTTGGGAGCACTGGACATTCCTGTAAGTC
TCGA-06-6390	FGFR3	D03U9ACXX110625:8:2304:13007:108632	F	1778520	1778521	2	0	0	CA***TCCCTCAGGACGTCCGCGGGAAGCCAAGCTTGTGGAG TTCGATTTCTTGGGAGCACTGGACATTCCTGTAAGTC
TCGA-06-6390	FGFR3	C01PRACXX110628:5:2108:1999:91559	F	1778518	1778521	4	0	0	GCCA***TCCCTCAGGACGTCCGCGGGAAGCCAAGCTTGTGG AGTTCGATTTCTTGGGAGCACTGGACATTCCTGTAAG
TCGA-06-6390	FGFR3	C01RDACXX110628:3:1308:1446:66311	F	1778515	1778521	7	0	0	CCGGCCA***TCCCTCAGGACGTCCGCGGGAAGCCAAGCTTG TGGAGTTCGATTTCTTGGGAGCACTGGACATTCCTGT
TCGA-06-6390	TACC3	D03U9ACXX110625:5:2205:12523:196352	R	1778514	1778521	8	1	0	CAGGAATGTCCAGTGCTACCAAGAAATCGAACTCCACAAGCT TGGGTTCCCGCGGACGTCCTCCGGGA***TGGCCGTG
TCGA-06-6390	TACC3	C01PRACXX110628:5:2103:6815:17943	R	1778514	1778521	8	0	0	CAGGAATGTCCAGTGCTCCCAAGAAATCGAACTCCACAAGCT TGGCTTCCCGCGGACGTCCTGAGGGA***TGGCCGGG
TCGA-06-6390	FGFR3	C01PRACXX110628:3:1204:10831:2928	F	1778512	1778521	10	0	0	TCCCCGGCCA***TCCCTCAGGACGTCCGCGGGAAGCCAAGC TTGTGGAGTTCGATTTCTTGGGAGCACTGGACATTCC
TCGA-06-6390	FGFR3	C01PRACXX110628:5:2204:6732:191360	F	1778512	1778521	10	0	0	TCCCCGGCCA***TCCCTCAGGANGTCCGCGGGAAGCCAAGC TTGTGGAGTTCGATTTCTTGGGAGCACTGGACATTCC
TCGA-06-6390	FGFR3	C01PRACXX110628:8:1308:2911:26590	F	1778511	1778521	11	0	0	GTCCCCGGCCA***TCCCTCAGGACGTCCGCGGGAAGCCAA GCTTGTGGAGTTCGATTTCTTGGGAGCACTGGACATTC
TCGA-06-6390	FGFR3	C01PRACXX110628:8:2207:4586:84017	F	1778509	1778521	13	0	0	CCGTCCCCGGCCA***TCCCTCAGGACGTCCGCGGGAAGCC AAGCTTGTGGAGTTCGATTTCTTGGGAGCACTGGACAT
TCGA-06-6390	TACC3	C01PRACXX110628:7:2205:11825:39734	R	1778501	1778521	21	0	0	TGCTCCCAAGAAATCGAACTCCACAAGCTTGGCTTCCCGCG GACGTCCTGAGGGA***TGGCCGGGGACGGCAGGGGGA
TCGA-06-6390	TACC3	C01PRACXX110628:6:1106:12159:179499	R	1778494	1778521	28	0	0	AAGAAATCGAACTCCACAAGCTTGGCTTCCCGCGGACGTCC TGAGGGA***TGGCCGGGGACGGCAGGGGGAGGGGCAT
TCGA-06-6390	TACC3	D03U9ACXX110625:4:2202:12501:40389	R	1778491	1778521	31	1	0	AAATCGAACTCCACAAGCTTGGCTTCCCGCGGACGTCCTGA GGGA***TGGCCGGGGGCGGCAGGGGGAGGGGCATAGG
TCGA-06-6390	FGFR3	C01RDACXX110628:3:1305:3044:13238	F	1778473	1778521	49	0	0	CTGGCCTGGTGCCACCCGCCTATGCCCCTCCCCCTGCCGTC CCCGGCCA***TCCCTCAGGACGTCCGCGGGAAGCCAA
TCGA-06-6390	TACC3	D03U9ACXX110625:5:2205:12523:196352	R	1778470	1778521	52	4	0	TCGTCCCGCGGACTTCCTGATGGA***TCGCCGGGGACGGCA GGGGGAGGGGCATAGGCGTGTGGCACCAGGCCAGCTC
TCGA-06-6390	TACC3	C01PRACXX110628:7:2205:11825:39734	R	1778469	1778521	53	1	0	CTTCCCGCGGACGTCCTGAGGGA***TGGCCGGGGACGGNA GGGGGAGGGGCATAGGCGGGTGGCACCAGGCCAGAGCC
TCGA-06-6390	FGFR3	D03U9ACXX110625:7:2106:4492:173350	F	1778464	1778521	58	0	0	GTGCTGGCTCTGGCCTGGTGCCACCCGCCTATGCCCCTCCC CCTGCCGTCCCCGGCCA***TCCCTCAGGACGTCCGCG
TCGA-06-6390	TACC3	C01PRACXX110628:5:2103:6815:17943	R	1778452	1778521	70	0	0	GAGGGA***TGGCCGGGGACGGCAGGGGGAGGGGCATAGG CGGGTGGCACCAGGCCAGAGCCAGCACTCACGTCGGTGG
TCGA-12-0826	TACC3	61C59AAXX100217:4:93:15133:6133	R	1778495	1778502	8	0	0	GGACAAGAGGGCAAGTGATCAGGTCTGACTGCCATCCCCTA ACACACACAGGGGGGCTAAGGGCAGGG***GAGGGGCA
TCGA-12-0826	TACC3	61C59AAXX100217:5:107:10675:16040	R	1778495	1778502	8	0	0	GGACAAGAGGGCAAGTGATCAGGTCTGACTGCCATCCCCTA ACACACACAGGGGGGCTAAGGGCAGGG***GAGGGGCA
TCGA-12-0826	FGFR3	61C59AAXX100217:5:108:1809:11295	F	1778494	1778502	9	0	0	ATGCCCCTC***CCCTGCCCTTAGCCCCCCTGTGTGTGTTAGG GGATGGCAGTCAGACCTGATCACTTGCCCTCTTGTC
TCGA-12-0826	FGFR3	61C59AAXX100217:5:82:13129:10637	F	1778490	1778502	13	0	0	GCCTATGCCCCTC***CCCTGCCCTTAGCCCCCCTGTGTGTGT TAGGGGATGGCAGTCAGACCTGATCACTTGCCCTCT
TCGA-12-0826	FGFR3	42MJNAAXX090813:6:80:691:1877#0	F	1778481	1778502	22	0	0	GTGCCACCCGCCTATGCCCCTC***CCCTGCCCTTAGCCCCC CTGTGTGTGTTAGGGGATGGCAGTCAGACCTGATCAC
TCGA-12-0826	TACC3	61C59AAXX100217:3:75:10586:12881	R	1778470	1778502	33	1	0	TGACTGCCATCCCCTAACACACACAGGGGGGCTAAGGGCAG GG***GAGGGGCATAGGCGGGGGGCACCAGGCCAGAGC
TCGA-12-0826	TACC3	61C59AAXX100217:4:114:5844:3161	R	1778470	1778502	33	1	0	TGACTGCCATCCCCTAACACACACAGGGGGGCTAAGGGCAG GG***GAGGGGCATAGGCGGGGGGCACCAGGCCAGAGC
TCGA-12-0826	TACC3	42MJNAAXX090813:5:70:888:108#0	R	1778466	1778502	37	3	0	TGCCATCCCCTAACACACACAGGGGGGCTAAGGGCAGGG*** GAGGGGCATAGGCGGGGGGCACCAGGACAGAGGCAGC
TCGA-12-0826	TACC3	61C59AAXX100217:3:55:4966:15975	R	1778451	1778502	52	5	0	CACACAGGGGGGCTAAGGGCAGGG***GAGGGGCATAGGCG GGGGGGACCAGGCCCGAGCCAGCACTCACGTCGGGGGG
TCGA-12-0826	FGFR3	42MJNAAXX090813:5:23:156:1150#0	F	1778447	1778502	56	0	0	GACGTCCACCGACGTGAGTGCTGGCTCTGGCCTGGTGCCA CCCGCCTATGCCCCTC***CCCTGCCCTTAGACCCCCTG
TCGA-12-0826	FGFR3	61C59AAXX100217:4:21:17613:20886	F	1778439	1778502	64	0	0	CTTACCGTGACGTCCACCGACGTGAGTGCTGGCTCTGGCCT GGTGCCACCCGCCTATGCCCCTC***CCCTGCCCTTAG
TCGA-12-0826	FGFR3	61C59AAXX100217:4:2:4279:6949	F	1778435	1778502	68	0	0	TGTCCTTACCGTGACGTCCACCGACGTGAGTGCTGGCTCTG GCCTGGTGCCACCCGCCTATGCCCCTC***CCCTGCCC
TCGA-19-5958	TACC3	C01RDACXX110628:6:1102:11157:101962	R	1778533	1778539	7	0	0	CGGGGGTGGGAGTGTGCGGGTGACCGGGGGTGGGAGTGT GCAGGTGACCTCCCTGGCCCTTAGCCCCCT***GCACTCT
TCGA-19-5958	TACC3	C01REACXX110629:2:2104:5009:98392	R	1778517	1778539	23	0	0	CGGGTGACCGGGGGAGGGAGTGTGCAGGGGACCTCCCTG GCCCTTAGCCCCCT***GCACTCTGGGGGGCAGGATGGCC
TCGA-19-5958	TACC3	C01PRACXX110628:7:2103:12434:91988	R	1778501	1778539	39	0	0	GGAGTGTGCAGGTGACCTCCCTGGCCCTTAGCCCCCT***GC ACTCTGGGGGGCAGGATGGCCGGGGACGGCAGGGGGA
TCGA-27-1835	TACC3	B06UCABXX110322:6:1103:9262:46754	R	1778586	1778595	10	1	0	GGGGAGGCTGCTGGTGGGCAGCTGACTGCGGGGACACTGG GAGGAAGCCTGGACCCTCAGCGAACT***TCGCCCAGCC
TCGA-27-1835	FGFR3	C00HWABXX110325:4:1201:20980:90877	F	1778567	1778595	29	0	0	ACAGCCTGGGCACAGAGGTGGCTGTGCGA***AGGTCGCTGA GGGTCCAGGCTTCCACCCAGTGTCCCCGCAGTCAGCT
TCGA-27-1835	TACC3	B06UCABXX110322:5:1108:14043:83287	R	1778564	1778595	32	0	0	TGACTGCGGGGACACTGGGTGGAAGCCTGGACCCTCAGCG ACCT***TCGCACAGCCACCTCTGTGCCCAGGCTGTGCC
TCGA-27-1835	TACC3	B097UABXX110405:4:2204:19445:88453	R	1778558	1778595	38	0	0	CGGGGACACTGGGTGGAAGCCTGGACCCTCAGCGACCT***T CGCACAGCCACCTCTGTGCCCAGGCTGTGCCCCAGAA
TCGA-27-1835	TACC3	B097UABXX110405:4:2201:20658:44401	R	1778557	1778595	39	2	0	GGGGACACTGGGTGGAAGCCTGGACCCTCAGCGACCT***TC GCACAGCCACCTCTGTGGCCAGGCTGTGCCACAGAAG
TCGA-27-1835	TACC3	B097UABXX110405:2:2104:15688:71022	R	1778555	1778595	41	0	0	GGACACTGGGTGGAAGCCTGGACCCTCAGCGACCT***TCGC ACAGCCACCTCTGTGCCCAGGCTGTGCCCCAGAAGGC
TCGA-27-1835	TACC3	C00HWABXX110325:6:2102:20394:42427	R	1778543	1778595	53	3	0	GAAGCCTGGACCCTCAGCGACCT***TCGCACAGCCACCTCT GTGCCCCGGCTGTGCCCCAGCCGGCCCGCCCCACACC
TCGA-27-1835	TACC3	B09V2ABXX110408:6:1203:18187:141862	R	1778543	1778595	53	0	0	GAAGCCTGGACCCTCAGCGACCT***TCGCACAGCCACCTCT GTGCCCAGGCTGTGCCCCAGAAGGCCCGCCCCACACC
TCGA-27-1835	TACC3	B09V2ABXX110408:8:1205:4774:81604	R	1778537	1778595	59	0	0	TGGACCCTCAGCGACCT***TCGCACAGCCACCTCTGTGCCC AGGCTGTGCCCCAGAAGGCCCGCCCCACACCTCAGCA
TCGA-27-1835	TACC3	C00HWABXX110325:2:1107:16168:23614	R	1778535	1778595	61	0	0	GACCCTCAGCGACCT***TCGCACAGCCACCTCTGTGCCCAG GCTGTGCCCCAGAAGGCCCGCCCCACACCTCAGCACT
TCGA-27-1835	TACC3	C00HWABXX110325:7:2107:1225:167363	R	1778530	1778595	66	0	0	TCAGCGACCT***TCGCACAGCCACCTCTGTGCCCAGGCTGT GCCCCAGAAGGCCCGCCCCACACCTCAGCACTCTGGG
TCGA-27-1835	TACC3	B097UABXX110405:2:2104:15688:71022	R	1778523	1778595	73	0	0	CCT***TCGCACAGCCACCTCTGTGCCCAGGCTGTGCCCCAG AAGGCCCGCCCCACACCTCAGCACTCTGGGGGGCAGG

Table S3 continuation

sample	gene split2	readi ID	direction split	hg18 start split2	hg18 stop split2	length2	mismatch2	gap2	seq mate
TCGA-06-6390	FGFR3	D03U9ACXX110625:2:1202:19578:90281	R	1708787	1708861	75	0	0	GACGTCCACCGACGTGAGTGCTGGCTCTGGCCTGGTGCCA
TCGA-06-6390	TACC3	C01PRACXX110628:3:1104:10052:66371	F	1708787	1708860	74	0	0	CCCGCCTATGCCCCTCCCCCTGCCGTCCCCGGCCAT
TCGA-06-6390	TACC3	C01PRACXX110628:5:1108:3119:22892	F	1708787	1708860	74	0	0	CAAGAGGGACTCAAGGACTTACAGGAATGTCCAGTGCTCCC
TCGA-06-6390	TACC3	D03U9ACXX110625:8:2304:13007:108632	F	1708787	1708860	74	0	0	AAGAAATCGAACTCCACAAGCTTGGCTTCCCGCGG
TCGA-06-6390	TACC3	C01PRACXX110628:5:2108:1999:91559	F	1708787	1708858	72	0	0	CAAGAGGGACTCAAGGACTTACAGGAATGTCCAGTGCTCCC
TCGA-06-6390	TACC3	C01RDACXX110628:3:1308:1446:66311	F	1708787	1708855	69	0	0	AAGAAATCGAACTCCACAAGCTTGGCTTCCCGCGG
TCGA-06-6390	FGFR3	D03U9ACXX110625:5:2205:12523:196352	R	1708787	1708854	68	4	0	ATAGGCCCTTAAAACAACTCGTTCCCTCAGACCACACACAAG
TCGA-06-6390	FGFR3	C01PRACXX110628:5:2103:6815:17943	R	1708787	1708854	68	0	0	ACAGTTCAAGAGGGACTCAAGGACTTACAGGAAT
TCGA-06-6390	TACC3	C01PRACXX110628:3:1204:10831:2928	F	1708787	1708852	66	0	0	TCAAGAGGGACTCAAGGACTTACAGGAATGTCCAGTGCTCC
TCGA-06-6390	TACC3	C01PRACXX110628:5:2204:6732:191360	F	1708787	1708852	66	1	0	CAAGAAATCGAACTCCACAAGCTTGGCTTCCCGCG
TCGA-06-6390	TACC3	C01PRACXX110628:8:1308:2911:26590	F	1708787	1708851	65	0	0	ACCACACACAAGACAGTTCAAGAGGGACTCAAGGACTTACA
TCGA-06-6390	TACC3	C01PRACXX110628:8:2207:4586:84017	F	1708787	1708849	63	0	0	GGAATGTCCAGTGCTCCCAAGAAATCGAACTCCAC
TCGA-06-6390	FGFR3	C01PRACXX110628:7:2205:11825:39734	R	1708787	1708841	55	0	0	GAGCTGGCCTGGTGCCACACGCCTATGCCCCTCCCCCTGCC
TCGA-06-6390	FGFR3	C01PRACXX110628:6:1106:12159:179499	R	1708787	1708834	48	0	0	GTCCCCGGCGATCCATCAGGAAGTCCGCGGGACGA
TCGA-06-6390	FGFR3	D03U9ACXX110625:4:2202:12501:40389	R	1708787	1708831	45	0	0	CCACCGACGTGAGTGCTGGCTCTGGCCTGGTGCCACCCGC
TCGA-06-6390	TACC3	C01RDACXX110628:3:1305:3044:13238	F	1708787	1708813	27	0	0	CTATGCCCCTCCCCCTGCCGTCCCCGGCCATCCCTC
TCGA-06-6390	FGFR3	D03U9ACXX110625:5:2205:12523:196352	R	1708787	1708810	24	4	0	CAAGAGCCTCAGACAGTGCATGAGGGACCCGAGACAGTGC
TCGA-06-6390	FGFR3	C01PRACXX110628:7:2205:11825:39734	R	1708787	1708809	23	0	0	GGCGAGGGAACAGCACAGCGGCCCCATGCCCCCAAC
TCGA-06-6390	TACC3	D03U9ACXX110625:7:2106:4492:173350	F	1708787	1708804	18	0	0	CAAGAGCCTCAGACAGTGCATGAGGGACCCGAGACAGTGC
TCGA-06-6390	FGFR3	C01PRACXX110628:5:2103:6815:17943	R	1708787	1708792	6	0	0	GGCGAGGGAACAGCACAGGGGCCCCATGCCCCCAAC
TCGA-12-0826	FGFR3	61C59AAXX100217:4:93:15133:6133	R	1707185	1707253	69	2	1	CGTTCCCTCAGACCACACACAAGACAGTTCAAGAGGGACTC
TCGA-12-0826	FGFR3	61C59AAXX100217:5:107:10675:16040	R	1707185	1707253	69	2	1	AAGGACTTACAGGAATGTCCAGTGCTCCCAAGAGA
TCGA-12-0826	TACC3	61C59AAXX100217:5:108:1809:11295	F	1707185	1707252	68	2	1	CCAGGAATAGAAAATATAGGCCCTTAAAACAACTCGTTCCCTC
TCGA-12-0826	TACC3	61C59AAXX100217:5:82:13129:10637	F	1707185	1707248	64	2	1	AGACCACACACAAGACAGTTCAAGAGGGACTCA
TCGA-12-0826	TACC3	42MJNAAXX090813:6:80:691:1877#0	F	1707185	1707239	55	2	1	GGCTCTGGCCTGGTGCCACCCGCCTATGCCCCTCCCCCTNC
TCGA-12-0826	FGFR3	61C59AAXX100217:3:75:10586:12881	R	1707185	1707228	44	2	1	CGTCCCCGGCCATCCCTCAGGACGTCCGCGGGAAGC
TCGA-12-0826	FGFR3	61C59AAXX100217:4:114:5844:3161	R	1707185	1707228	44	2	1	GCCCTGCCCGCAGGTACATGATCATGCGGGAGTGCTGGCAT
TCGA-12-0826	FGFR3	42MJNAAXX090813:5:70:888:108#0	R	1707185	1707224	40	2	1	GCCGCGCCCTCCCAGAGGCCCACCTTCAAGCAGCT
TCGA-12-0826	FGFR3	61C59AAXX100217:3:55:4966:15975	R	1707185	1707209	25	2	1	CTGGCATGCCGCGCCCTCCCAGAGGCCCACCTTTAAGCAGC
TCGA-12-0826	TACC3	42MJNAAXX090813:5:23:156:1150#0	F	1707185	1707205	21	2	1	TGGTAGAGGGCCTGGACCGTGTCCTTACCGTGACG
TCGA-12-0826	TACC3	61C59AAXX100217:4:21:17613:20886	F	1707185	1707197	13	0	1	TAAAACAACTCGTTCCCTCAGACCACACACAAGACAGTTCAA
TCGA-12-0826	TACC3	61C59AAXX100217:4:2:4279:6949	F	1707185	1707193	9	0	1	GAGGGACTCAAGGACTTACAGGAATGTCCAGTGC
TCGA-19-5958	FGFR3	C01RDACXX110628:6:1102:11157:101962	R	1707202	1707270	69	1	0	CACGGCCATCCCTCAGGACGTCCGCGGGAAGCCAAGCTTG
TCGA-19-5958	FGFR3	C01REACXX110629:2:2104:5009:98392	R	1707202	1707254	53	3	0	TGGAGTTCGATTTCTTGGGAGCACTGGACATTCCTG
TCGA-19-5958	FGFR3	C01PRACXX110628:7:2103:12434:91988	R	1707202	1707238	37	1	0	GGCATGCCGCGCCCTCCCAGAGGCCCACCTTCAAGCAGCT
TCGA-27-1835	FGFR3	B06UCABXX110322:6:1103:9262:46754	R	1709397	1709462	66	2	0	GGTGGAGGACCTGGACCGTGTCCTTACCGTGACGTC
TCGA-27-1835	TACC3	C00HWABXX110325:4:1201:20980:90877	F	1709397	1709443	47	0	0	GGCATGCCGCGCCCTCCCAGAGGCCCACCTTCAAGCAGCT
TCGA-27-1835	FGFR3	B06UCABXX110322:5:1108:14043:83287	R	1709397	1709440	44	0	0	GGTGGAGGACCTGGACCGTGTCCTTACCGTGACGTC
TCGA-27-1835	FGFR3	B097UABXX110405:4:2204:19445:88453	R	1709397	1709434	38	0	0	CGGCATGCCGCGCCCTCCCAGAGGCCCACCTTCAAGCAGCT
TCGA-27-1835	FGFR3	B097UABXX110405:4:2201:20658:44401	R	1709397	1709433	37	0	0	GGTGGAGGACCTGGACCGTGTCCTTACCGTGACGTCCACCGACG
TCGA-27-1835	FGFR3	B097UABXX110405:2:2104:15688:71022	R	1709397	1709431	35	0	0	CCTGCCCCCCAGAGTGCTGAGGTGTGGGGCGGGCCTTCTG
TCGA-27-1835	FGFR3	C00HWABXX110325:6:2102:20394:42427	R	1709397	1709419	23	0	0	GGGCACAGCCTGGGCACAGAGGTGGCTGTGCGAAGG
TCGA-27-1835	FGFR3	B09V2ABXX110408:6:1203:18187:141862	R	1709397	1709419	23	0	0	GCAGGTACATGATCATGCGGGAGTGCCGGCATTTCGGGACC
TCGA-27-1835	FGFR3	B09V2ABXX110408:8:1205:4774:81604	R	1709397	1709413	17	0	0	TTCCCTCGGGCCACCCTCTTCCGGTTGTTGTGGGC
TCGA-27-1835	FGFR3	C00HWABXX110325:2:1107:16168:23614	R	1709397	1709411	15	0	0	GCAGGTACATGATCATGCGGGAGTGCTGGCATGCCGCGCCC
TCGA-27-1835	FGFR3	C00HWABXX110325:7:2107:1225:167363	R	1709397	1709406	10	0	0	TCCCCGAGGACCACCTTCCAGCAGCCGGGGGAGGG
TCGA-27-1835	FGFR3	B097UABXX110405:2:2104:15688:71022	R	1709397	1709399	3	0	0	CCCGAATAAGGTGGGAAGCGGCGGGGCTCACTCCTGAGCG
									CCCTGACCGCAGGTACATGAGCATGCGGGAGTGGCG
									CGTGTCCTTACCGTGACGTCCACCGACGTGAGTGCTGGCTC
									TGGCCTGGTGCCACCCGCCTATGCCCCTCCCCCTG
									ACATGATCATGCGGGAGTGCTGGCATGCCGCGCCCCCCCAG
									AGGCCCACCTTCAAGCAGCTGGTGGAGGACCTGGA
									GCCTTCTGGGGCACAGCCTGGGCACAGAGGTGGCTGTGCG
									AAGGTCGCTGAGGGTCCAGGCTTCCACCCAGTGTCC

Table S4. IDH1 and IDH2 status and clinical data of GBM patients harboring FGFR-TACC gene fusions

Samples	Type	Time	Status	Age at initial pathologic diagnosis	IDH1-2 status (Sanger)	IDH1-2 status (exome)
TCGA-12-0826	FGFR3-TACC3	845	DEAD	38	WT	WT
TCGA-27-1835	FGFR3-TACC3	648	DEAD	53	NA	WT
TCGA-19-5958	FGFR3-TACC3	164	ALIVE	56	NA	WT
TCGA-06-6390	FGFR3-TACC3	163	DEAD	58	WT	WT
GBM-22	FGFR3-TACC3	390	DEAD	60	WT	NA
GBM-1123	FGFR3-TACC3	NA	DEAD	62	WT	NA
GBM-51	FGFR1-TACC1	NA	NA	NA	WT	NA

Time = Survival (days after diagnosis)
Sanger = analysis done by Sanger sequencing of genomic DNA
Exome = alnalysis done by the SAVI (Statistical Algorithm for Variant Identification), an algorithm developed to detect point mutation in cancer (BRAF Mutations in Hairy-Cell Leukemia, Tiacci E et al. The New England Journal of Medicine 2011 Jun 16;364(24):2305-15)
NA = Not Available
WT = Wild type sequence for R132 and R172 of IDH1 and IDH2, respectively

Table S5: *In vitro* and *in vivo* transformation assays

Cell line	Vector	FGFR3	TACC3	F1-T1 Fusion	F3-T3 Fusion	F3-T3-K508MFusion
Rat1 (# soft agar colonies)	0	0	0	225.3±10.0	198.7±8.0	0
Balb 3T3 (# soft agar colonies)	0	0	0	n.d.	45.5±8.9	n.d.
Rat1 A (# mice with tumor)	0/5	0/5	0/5	n.d.	5/5	n.d.
*Ink4A;Arf-/-*Astrocytes (# mice with tumor)	0/9	0/5	0/5	8/8	12/12	0/8

n.d.: not done

Table S6: Chromosomal segregation defects induced by FGFR-TACC fusions

Cell line	Metaphases inspected	Cells with segregation defects (%±SD)	Metaphases with misaligned chromosomes (%±SD)	Anaphases with lagging chromosomes (%±SD)	Anaphases/telophases with chromosome bridges (%±SD)
Rat1A Vector	150	9.5±3.8	2.3±1.7	2.4±0.9	5.4±2.4
Rat1A FGFR3-TACC3	150	27.4±3.9	8.0±2.6	8.0±1.0	11.2±0.7
Rat1A FGFR1-TACC1	100	45.5±3.1	5±2.8	10±1.4	31.5±4.9
Ink4A;ARF-/- Vector	100	7.3±1.5	2.2±1.5	2.0±0.7	3.3±0.6
Ink4A;ARF-/- FGFR3-TACC3	100	18.3±1.5	6.0±1.1	6.5±1.3	11.2±0.7

Table S7: Analysis of chromosomal number

Cell line	Number of cells counted	Percent aneuploidy	Range	Mean number	Average variation from mean number	*p*- value
Rat1A Vector	100	27	35-43	41.2	1.2	
Rat1A FGFR3	100	33	35-44	42.1	1.3	n.s.
Rat1A TACC3	100	41	34-46	40.7	1.1	n.s.
Rat1A FGFR3-TACC3	100	69	35-73	43.8	3.1	<0.0001
Human Astrocytes Vector	100	8	42-46	45.85	0.28	
Human Astrocytes FGFR3-TACC3	100	42	28-48	42.24	3.33	<0.001

Table S8. Chromosome analysis by SKY of 20 cells from the GSC-1123 culture

Cell #	Chr #	+1	+2	+3	t(3;14)	+4	(-4)	del(4)	+5	+6	+7	del(7)	+8	-9	+9	-10	+10	+11
1	**97**	2	2	2		2		1	2	2	4		2		2			2
2	**51**										1					1		
3	**49**										1					1		
4	**50**										1					1		
5	**49**										1					1		
6	**86**	2	2	2		2			2		3		1		1			2
7	**95**	2	2	2		2			1	2	4		2		2			2
8	**98**	2	3	2	1	2			1	2	4		3		1			2
9	**86**	2	1	1	1	1			1	1	6		2		3		1	1
10	**44**			1	1		1				1	1		1		1		
11	**49**										1	1				1		
12	**49**										1					1		
13	**98**	2	2	2	2				2	2	4		2		2			2
14	**49**										1					1		
15	**48**										1					1		
16	**51**										1					1		
17	**49**										1					1		
18	**50**										1	1				1		
19	**49**										1					1		
20	**49**										1					1		

Table S8 continuation

Cell #	Chr #	+12	+13	del(13)	-14	+14	+15	-16	+16	+17	+18	+19	+20	-21	+21	-22	+22	+X
1	**97**	2	2	2		2	2		2	2	3	4	4		2		2	2
2	**51**		2	2							1	1	1					
3	**49**			1							1	1	1					
4	**50**			1							1	1	1					1
5	**49**			1							1	1	1					
6	**86**	2	2	2		2	2			2	4	3	3		1			2
7	**95**	2	2	2		2	2		2	2	4	2	4		2		2	2
8	**98**	2	2	2		2	2		2	2	3	4	4		3		2	2
9	**86**	2	2	2					2	1	4	3	1		2		1	2
10	**44**				1			1			1		1			1		
11	**49**										1	1	1					
12	**49**			1							1	1	1					
13	**98**	2	2			2	2		2	2	4	4	4		2	2		2
14	**49**			1							1	1	1					
15	**48**										1	1	1	1				
16	**51**			1		1					1						2	1
17	**49**		1								1	1	1					
18	**50**		1	1							1	1	1					
19	**49**										1	1	1					
20	**49**			1							1	1	1					

Table S9: Analysis of chromosomal number in Rat1A cells treated with the FGFR3 inhibitor PD173074

Cell line	Number of cells counted	Percent aneuploidy	Range	Mean number	Average variation from mean number	*p*- value
Rat1A Vector DMSO	100	38	37-55	41.7	1.10	
Rat1A Vector PD173074	100	39	37-46	42.0	0.77	n.s.
Rat1A FGFR3-TACC3 DMSO	100	88	31-96	43.7	4.11	<0.0001
Rat1A FGFR3-TACC3 PD173074	100	49	31-48	42.0	1.28	<0.0001